Received: 28 July 2025 | Accepted: 25 April 2026

DOI: 10.1002/tpg2.70250

The Plant Genome

ORIGINAL ARTICLE

Genome-wide association studies of a pea germplasm reveal novel markers and candidate genes implicated in resistance to *Fusarium oxysporum* f. sp. *pisi* races 1 and 2

Osman Zakaria Wohor[1,2] | **Diego Rubiales**[1] | **Nicolas Rispail**[1]

[1]Institute for Sustainable Agriculture, CSIC, Cordoba, Spain

[2]Savanna Agriculture Research Institute, CSIR, Tamale, Nyankpala, Ghana

Correspondence
Osman Zakaria Wohor, Institute for Sustainable Agriculture, CSIC, Avda. Menéndez Pidal s/n, 14004, Cordoba, Spain.
Email: owohor@ias.csic.es

Assigned to Associate Editor Manish Pandey.

Funding information
Horizon Europe, Grant/Award Numbers: 101081878 BELIS, 101135314 COUSIN; International Crops Research Institute for the Semi-Arid Tropics (ICRISAT), Grant/Award Number: TLIII; AGENCIA ESTATAL DE INVESTIGACIONES, Grant/Award Numbers: PID2020-113153RB-I00, PID2023-146215OB-I00

Abstract

Pea (*Pisum sativum* L.) is an essential legume crop cultivated globally as food and feed. However, its production is greatly constrained by *Fusarium oxysporum* f. sp. *pisi* (*Fop*). Breeding for resistance is the most efficient management strategy, but the genetic foundation of *Fop* resistance remains unclear. Previous quantitative trait loci mapping has located several genomic regions associated with resistance to *Fop*. However, the large marker-trait distances hampered the implementation of marker-assisted selection. To unravel candidate genes for *Fop* races 1 and 2, diversity array technology (DArT) markers were applied to 324 pea core collections for a genome-wide association study (GWAS). Phenotyping of the collections were performed under controlled growth chamber conditions with three independent experiments in a 324 × 3 × 7 factorial design. The collections were inoculated, and disease incidence was quantified over time using the area under the disease progress curve as the primary phenotypic measure for analyses. Phenotypic results revealed quantitative response and implicated wild accessions and landraces as favorable reservoirs of *Fop* resistance. GWAS using 26,045 DArT markers with three different models detected 15 marker-trait associations (MTAs) for *Fop* race 1 and 27 MTAs for *Fop* race 2 resistance. MTAs were scattered across six pea chromosomes, with several of them located within the confidence interval of four previous *Fop* resistance loci—thereby refining their location. In addition, 28 potential candidate genes were identified near associated markers involved in *Fop* resistance, including genes encoding a reverse transcriptase, exocyst and conserved oligomeric Golgi complex

Abbreviations: ATP, adenosine triphosphate; AUDPC, area under disease progress curve; BIC, Bayesian information criterion; BLINK, Bayesian information and linkage-disequilibrium iteratively nested keyway; BLUP, best linear unbiased prediction; COG, conserved oligomeric Golgi complex; DAPC, discriminant analysis of principal components; DArT, diversity array technology; DArTseq, diversity arrays technology sequencing; DSI, disease severity index; FarmCPU, fixed and random model circulating probability unification; FDR, false discovery rate; Fnw, Fusarium near wilt; FW, Fusarium wilt; GWAS, genome-wide association study; LD, linkage disequilibrium; LG, linkage group; MAB, marker-assisted breeding; MAS, marker-assisted selection; MLM, mixed linear model; MTA, marker-trait association; PCs, principal components; PVE, phenotypic variance explained; Q–*Q*, quantile–quantile; QTL, quantitative trait locus; RCBD, randomised complete block design; SNP, single-nucleotide polymorphism.

subunits, a FERONIA-like receptor kinase, homoserine kinase, a heat shock 70 protein, adenosine triphosphate transporters, and multiple transcription factors and plant defense-related proteins. These putative genes and molecular pathways provide a foundation for the sustainable management of *Fop*.

Plain Language Summary

Breeding pea for disease resistance is one of the most effective and sustainable strategies to improve production and food security. This study builds on earlier related studies and provides a strong foundation for future understanding the functions of valuable genetic factors (genes) involved in *Fusarium oxysporum* f. sp. *pisi* (*Fop*) disease resistance. For the first time, a large phenotyping and genotyping information of pea is used in scanning the genome (genome-wide association study) to identify genes connected to *Fop* races 1 and 2 disease resistance. We found 42 linked markers and 28 potential genes involved in *Fop* resistance. We also found new evidence of quantitative resistance to *Fop* race 1 and confirmed the quantitative inheritance of *Fop* race 2 as previously reported. This knowledge provides valuable insight for future pea improvement toward food security.

1 | INTRODUCTION

Pea (*Pisum sativum* L.) is a temperate annual grain legume, cultivated globally as food and feed (Rubiales et al., 2019). The genetics of pea is complex with a large genome of 4.45 Gb, arranged into seven pairs of homologous chromosomes ($2n = 2x = 14$) rich in repetitive sequences (Kreplak et al., 2019; N. Liu et al., 2024; Smýkal et al., 2012). This complexity, along with its autogamous nature, limits genetic diversity compared to outcrossed crops—posing challenges for developing pea genomic resources (Pandey et al., 2021). The current taxonomy of the genus *Pisum* remains debatable, but it is generally accepted to contain three primary species: *P. sativum* L., *Pisum fulvum* Sibth & Sm., and *Pisum abyssinicum* A. Braun (Smýkal et al., 2012). However, recent studies further categorized *P. sativum* into six subspecies (Rispail et al., 2023). Landraces and wild species are known to harbour valuable traits—thus, utilization of gene bank materials would facilitate improved genetic bottlenecks (Rubiales et al., 2023). Pea is a cheap source of protein, serving a valuable soil amendment function through nitrogen fixation, green manuring, and the liberation of useful micronutrients for successive rotational crops' uptake (Singh et al., 2022; Windsor et al., 2024; Zander et al., 2016). Thus, pea can attain cost-efficient yields with minimal chemical fertilizer inputs and less environmental carbon footprint (Rubiales, 2023). Accordingly, global demand for pea has continued to increase over the years, but production remains unstable. Global production estimates of dry pea in 2021/2022 were 14.2 million metric tonnes (MMT) on a harvested area of 7.2 million hectares (Mha), which recently declined to 13.8 MMT on an area of 7.4 Mha for the 2023/2024 season (FAOSTAT, 2025). This decline in production despite a 2.8% increase in cultivated area, likely reflects the influence of biotic stresses, poor agronomic management, and climatic constraints.

Low and variable pea yields are mainly due to its high susceptibility to soilborne diseases, which adversely limit its production. Among them, Fusarium wilt (FW), caused by *Fusarium oxysporum* Schlecht f.sp. *pisi* (van Hall) Snyd. & Hans (*Fop*) is a major threat that can induce about 80%–100% yield penalty if thresholds are exceeded (Wohor et al., 2022). *Fop* spore germination and host infection are induced by host root exudates. *Fop* infection symptoms are mostly progressive from lower to upper leaves, resulting in dwarfism, yellowing, wilting, and ultimately plant death (Bani et al., 2012; Verma et al., 2025). The ability of *Fop* to induce different responses in various pea cultivars and their genetic characteristics allowed identification of four main races (1, 2, 5, and 6) (Infantino et al., 2006). Races 1 and 2 have global significance, while races 5 and 6 were thought to be limited to the Washington region of the United States (Infantino et al., 2006) but are expanding, as race 5 has recently been reported in China (Deng et al., 2022). Similar to other soilborne diseases, *Fop* exhibits high survival plasticity, persisting for many years in the soil as specialised adaptive chlamydospores, making its control challenging (Bani et al., 2018; Wohor et al., 2022). The similarity of FW symptoms to those of other diseases and certain nutrient deficiencies further complicate its management strategy. Once the pathogen enters the soil, there is no satisfactory control measure, as most of the available control

methods are largely ineffective and potentially detrimental to the environment (Wohor et al., 2022). The most efficient and sustainable management of *Fop* is through the identification and incorporation of resistance genes into adapted pea cultivars. Breeding for resistance requires the deployment of genetic alleles from landraces or wild relatives to broaden genetic variability of modern cultivars (Rubiales, 2023). Different gene-bank materials have been deployed, along with standard genotyping and phenotyping methods, to decode valuable *Fop*-resistant alleles (Wohor et al., 2022). Previous screening in pea reported that resistance to races 1, 5, and 6 are monogenic in nature and controlled by single race-specific genes (Infantino et al., 2006), while resistance to race 2 is quantitative (Bani et al., 2012; McPhee et al., 2012). Monogenic resistance against races 1, 5, and 6 has been successfully incorporated into cultivars (McPhee et al., 1999; Porter et al., 2014). Nonetheless, these monogenic sources of resistance are at risk of breakdown due to the constant evolution of the pathogen that already led to the emergence of the distinct races and pathogenic variants of *Fop* (Infantino et al., 2006; Neumann & Xue, 2003).

The efficiency of pea breeding is being enhanced by the cost reduction and rapid advancement of novel high-throughput genomic techniques (Tayeh et al., 2015; Verma et al., 2025). Although pea lagged behind other legumes in disease quantitative trait locus (QTL) discovery, the recent well-annotated, high-resolution, pea reference genomes present a great resource to accelerate resistance and marker-assisted breeding (MAB) (Gali, Tar'an, et al., 2019; N. Liu et al., 2024; Yang et al., 2022). MAB has the potential to aid visual phenotyping and genotyping capabilities to reduce breeding cycles (Pandey et al., 2021). Genetic markers are the most preferred markers for MAB because they are less susceptible to environmental variations (Nogué et al., 2016; Tayeh et al., 2015). Hence, markers have been developed and successfully deployed to measure genetic variation and improve pea polygenic traits (Gali et al., 2018; Sindhu et al., 2014). Analysis of bi-parental populations segregating for *Fop* race 1 resistance identified a single resistance locus named *Fw* on pea linkage group (LG) III (chromosome 5) and identified several tightly linked markers located in a 1.2cM window, allowing the development of selectable markers for marker-assisted selection (MAS) (Jain et al., 2015). The use of a bi-parental population segregating for *Fop* race 5 resistance also detected a single locus, *Fwf*, within a window of 9.1 cM on LG II (chromosome 6) (Coyne et al., 2000). Most recently, a dominant gene (*FwS1*) responsible for resistance to race 5 and tightly linked to *Fwf* has also been identified and finely mapped on chromosome 6 within a genetic distance of 91.4 kb (Deng et al., 2024). In turn, two minor loci (*Fnw3.1* and *Fnw3.2*, Fusarium near wilt) and a major locus (*Fnw4.1*) on LG III and IV of chromosomes 5 and 4, respectively, were reported for resistance to race 2, although no selectable markers have been proposed yet (McPhee et al., 2012).

These QTL techniques have been resourceful, but the low allelic variation contained in the bi-parental populations, coupled with the low marker density are bottlenecks in QTL analysis, hindering the precision and efficiency of identifying genetic loci associated to traits (Myles & Wayne, 2008). High-throughput genomic approaches such as genome-wide association studies (GWASs) complement QTL mapping by providing higher-resolution marker detection of genomic loci underlying quantitative traits (Resende et al., 2014). GWAS captures allele effects that explain trait variation in diverse populations, through linkage disequilibrium (LD) between markers and causal loci (Myles & Wayne, 2008). Since population structure strongly influences marker-trait associations, robust models are essential to account for genetic diversity and ensure accurate detection of true associations (Crosta et al., 2023; Li et al., 2026; Wohor et al., 2025). The utilization of numerous markers enables detailed genome coverage to overcome the constraints of bi-parental populations (Susmitha et al., 2023). Diversity Arrays Technology sequencing (DArTseq) markers are abundant, allowing for extensive genome coverage, making them well-suited for GWAS (Pandey et al., 2021). DArTseq generates single-nucleotide polymorphism (SNP) and SilicoDArT markers through restriction enzyme-mediated genome complexity reduction and sequencing of the restriction fragments

Core Ideas

- Efficient evaluation and strategic utilization of diverse germplasm are essential for identification and harnessing gene variants underlying key biotic traits.
- Phenotyping a pea core collection for *Fusarium oxysporum* f.sp. *pisi* (*Fop*) resistance reveal substantial variation in response to *Fop* races 1 and 2, confirming the quantitative nature of their resistance.
- The study represents the first genome-wide association studies implemented to elucidate *Fop* resistance in pea.
- Diversity array technology markers demonstrate robustness for detecting 28 candidate genes involved in *Fop* races 1 and 2 resistance.
- Elucidated putative genes and molecular pathways provide a foundation for future *Fop* gene functional studies to facilitate the incorporation of resistant loci through marker-assisted and genomic selection.

(Gali et al., 2018). In pea, DNA-based markers successfully aided the identification of novel marker-trait associations (MTAs) for disease resistance through GWAS (Desgroux et al., 2016; Leprévost et al., 2023; Osuna-Caballero et al., 2024a; Osuna-Caballero et al., 2024b; Rodriguez-Mena et al., 2025; Wohor et al., 2025). In addition, GWAS identified 17 SNPs associated with *Fop* race 2 resistance in grass pea (*Lathyrus sativus*), seven of which were mapped to pea chromosomes 1, 6, and 7 (Sampaio et al., 2021). Despite these achievements, the genomic regions conferring resistance to the main races of *Fop* remain large—impeding identification of the responsible genes. Reviews on genetic and molecular approaches to *Fop* reveals that GWAS has not yet been implemented for this pathogen in pea (Ghosal & Datta, 2025; Verma et al., 2025). To improve the understanding of the genetic architecture of *Fop* resistance, the present study seeks to phenotype a genotyped pea core collection and perform a GWAS analysis to elucidate DArT markers and putative candidate genes/pathways significantly linked to *Fop* races 1 and 2 resistance. This study is expected to enhance the efficient implementation of future functional genetic analysis of candidate genes involved in *Fop* resistance to facilitate MAS in pea breeding and enhance food security.

2 | MATERIALS AND METHODS

2.1 | Plant material

The plant material used in this study consisted of a diverse core collection of 324 pea accessions of worldwide origin assembled at the Institute for Sustainable Agriculture, CSIC, Córdoba, Spain (Table S1). The panel was initially curated from a large *Pisum* spp. collection of > 3000 accessions provided by USDA (Department of Agriculture), JIC (John Innes Center), CRF (Centro Nacional de Recursos Fitogenéticos), CGN (CPRO-DLO), IPK (Leibniz Institute of Plant Genetics and Crop Plant Research), and ICARDA (International Center for Agricultural Research in the Dry Areas) (Rispail et al., 2023). The core collection was carefully selected to represent most of the existing pea genetic diversity, including accessions from all recognized *Pisum* species and subspecies. The accession #251 (PI 505059), known for its susceptibility to *Fop* races 1 and 2, was included in the collection as a check. The genetic diversity of the core collection was characterized to reveal their high genetic diversity and suitability for GWAS (Rispail et al., 2023).

2.2 | Fungal materials and plant inoculation

The fungal materials used to screen the pea collection consisted of two *Fop* isolates, F79 and F42, belonging to the pathogenic *Fop* races 1 and 2, respectively. These isolates were maintained in micro-conidial suspension at −80°C in 30% glycerol and prepared for inoculation by culturing in potato dextrose broth at 28°C under constant agitation (170 rpm). The inoculum concentration was adjusted to 5×10^6 microconidia spores mL^{-1} of water using the root-dip method by Bani et al. (2012). This inoculation procedure involves the cleaning and trimming of pea roots to one-third and dipping them into the *Fop* spore suspension for 5 min before transplanting. Control plants were treated identically but immersed in sterile water to homogenize treatments.

2.2.1 | Experiment layout

All experiments were performed under controlled conditions. Pea seeds were subjected to surface sterilization, scarification, and cold treatment at 4°C for 3 days to break dormancy and synchronize germination. Pre-germination was initiated in a growth chamber at 21°C for 48 h using wet tissue paper wrapped with aluminum foil to ensure complete darkness. Germinated seeds were then planted in sterile vermiculite-filled pots in a growth chamber with 16/8 h light-darkness cycle, a 26 ± 2°C temperature, and 200 µmol m-2 s-1 illumination. After a week (two-leaf stage), seedlings were inoculated with *Fop* using the root dipping method, followed by transplanting into fresh sterile vermiculite-filled pots. Subsequently, inoculated seedlings were maintained under the same growth chamber conditions. Plants were watered regularly with tap water and applied with half-strength Hoagland nutrient solution once a week (Hoagland & Arnon, 1938). The experiment involved three plants per accession in a randomised complete block design (RCBD) with 324 accessions, three replicates, and seven block units per replicate ($324 \times 3 \times 7$ factorial). The whole experiment was repeated three times independently (E1, E2, and E3) for each *Fop* isolate, resulting in a total of nine plants evaluated per accession and isolate.

2.3 | Phenotyping

Disease symptoms assessment was extensively carried out among the pea collection by evaluating disease severity every 3 days from the 7th to the 30th day after inoculation (Bani et al., 2012). Infection severity was quantified as the percentage of symptomatic leaf per plant, estimated from the evaluation of each plant leaf with a five-point scale at leaf level and 100-point rating scale at whole plant level (Figure 1; Figure S1). Disease severity index (DSI) for each plant was then calculated by integrating the disease ratings of the scored leaves using the following equation:

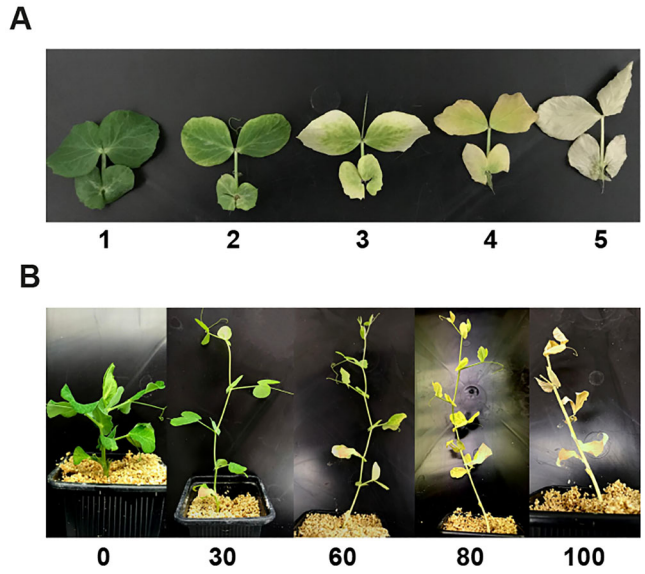

FIGURE 1 Disease ratings scale based on (A) the 5-point scale at leaf level (1 = no disease, 2–3 = moderate disease, 4–5 = full disease rate) and (B) 100-point scale at whole plant level (0 = no infection, 30–60 = moderate infection, 80 = severe infection, and 100 = plant death).

$$\text{DSI} = \frac{0.5N_1 + 1N_2}{N_t} \times 100$$

where N_1 is the number of leaves at stages 2 and 3, N_2 is the number of leaves at stages 4 and 5 and N_t is the total number of leaves (Figure 1). Rated data were standardized with their respective controls to eliminate false positive scores.

The periodic DSI was then used to estimate the area under disease progress curve (AUDPC) using the following formula:

$$\text{AUDPC} = \sum_{i=1}^{n} \left(\frac{x_i + x_{i+1}}{2} \right) \times \left(t_{i+1} - t_i \right)$$

where n is total number of observations, x_i is the estimated proportion of disease severity at date i, x_{i+1} is the estimated proportion of disease severity at date $i + 1$, and $t_{i+1} - t_i$ the number of days between scoring dates i and $i + 1$ (Bani et al., 2012).

Before further analysis, AUDPC values from the three independent inoculated experiments (E1, E2, and E3) of the *Fop* race 1 and 2 were compared and combined to obtain the best linear unbiased predictions (BLUPs) with the *metan* package in R version 4.2.2 (Olivoto & Lúcio, 2020) considering the mixed linear model (MLM):

$$Y_{ijk} = \mu + E_i + G_j + (G \times E)_{ij} + \epsilon_{ijk}$$

where Y_{ijk} is the observed phenotypic response of the jth genotype (1, 2, …,324 genotypes) in the ith environment (E1, E2, and E3 environments) and Kth replicate, μ is the overall mean (fixed effect), E_i is the fixed effect of environment, $G_j \sim N(0, \sigma^2_G)$ is random effect of genotype, $(G \times E)_{ij} \sim N(0, \sigma^2_{GE})$ is the random genotype x environment interaction, and $\epsilon_{ijk} \sim N(0, \sigma^2_e)$ is the residual error associated with genotype × environment interaction.

BLUPs are predictions of random effects and represent the genetic component of each genotype's performance, adjusted for random variation and shrinkage toward the population mean, but have an advantage of reducing environmental noise and design variance (Robinson, 1991). Estimated BLUPs were then used for all subsequent analysis. Comparison between accessions was performed for each *Fop* isolates independently by one-way analysis of variance (ANOVA). Prior to ANOVA, normal distribution and homogeneity of the data were assessed by Shapiro–Wilk and Pearson's matrix, respectively, by visual examination of scatter plots and histogram of residuals. These tests revealed the heteroscedasticity of the data, while the normality presumption stands true. Therefore, Welch's correction was applied in the ANOVA to account for the heteroscedasticity of the data. Whenever the tests were statistically significant ($p \leq 0.05$), mean separation between accessions was determined by *post hoc* pairwise comparison test at 95% confidence level using Games-Howell's test. Welch's ANOVA and Games-Howell's test were performed with the packages *rstatix* in R (Kassambara, 2023). The correlation between estimated means was assessed using the "corr_plot" function of the *metan* R package to determine Pearson's correlation matrix, and their broad sense heritability's estimated for each trait by the ratio of genotypic variance to phenotypic variance (Olivoto & Lúcio, 2020).

2.4 | Genotyping

The genotyping of the collection was performed in Rispail et al. (2023). In brief, genotyping of the 324-pea core collection was conducted following DArTseq protocols by extracting DNA from leaves of week-old seedlings (20 per accession) and analyzed using the high-density Pea DArTSeq 1.0 array. Genomic data were cleaned to eliminate low-quality and non-polymorphic markers; DArT markers with >20% missing data, <5% minor allele frequency, or heterozygosity >10% were excluded. The resulting 26,045 polymorphic Silico DArT markers were retained for the final analysis as they provided a more complete genome cover than the SNPs dataset markers (Rispail et al., 2022). These silico-DArT markers were then aligned to the Caméor (V1a) and Zhongwan 6 (ZW6) reference genomes of pea (Kreplak et al., 2019; Yang et al., 2022).

2.5 | Assessment of population structure

The genetic structure of the pea diversity panel was estimated in R by discriminant analysis of principal components

(DAPC), implemented in the ADEGENET 2.1.11 package (Jombart, 2008; Jombart et al., 2010; R Core Team, 2024). To select the optimal number of clusters (K), a sequential k-means analysis was implemented from $K = 1$ to $K = 30$ using the function "find.cluster" of the ADEGENET package in R (Jombart et al., 2010). Selection of the optimal number of clusters was based on the Bayesian information criterion (BIC) (Figure S2) and the automatic selection with the model "goodness of fit" criterion. The number of principal components (PCs) to include in the DAPC analysis was initially set at 13 according to the optimization of the "a-score" that measure the trade-off between discrimination power and data overfitting. Accordingly, the number of discriminant axes was set to six that was sufficient to explain a significant portion of the variance.

2.6 | Genome-wide association studies

The GWAS models were based on the 26,045 DArTseq markers that were homogeneously distributed across the pea genome (Rispail et al., 2022) and on the robust phenotypic evaluation of the pea core collection for *Fop* races 1 and 2 resistance. The genotypic data entailed genetic marker information, with the PCs serving as covariance and the K-matrix as predetermined variances—while the observed phenotypic information in the GWAS model was based on the estimated BLUP means. GWAS was implemented in R with the GAPIT 3.0 package (Wang & Zhang, 2021), a robust tool for streamlining association mapping workflow. Population structure information, kinship matrix, and LD were considered in the GWAS models to mitigate confounding effects. The scree plot selection procedure (Figure S3) was used to determine the optimal number of PCs required to effectively correct for population structure. GWAS was conducted using three different models: MLM (Yu et al., 2006), Fixed and random model Circulating Probability Unification (FarmCPU) (X. Liu et al., 2016), and Bayesian information and Linkage-disequilibrium Iteratively Nested Keyway (BLINK) (Huang et al., 2019). These models were chosen based on statistical merit and their complementarity to capture the most significant variants of small and large effects for robust gene calling (Wang et al., 2022). Significant associations were extracted by the Bonferroni correction as the primary threshold for validating DArTseq markers—to minimize false positives (Bland & Altman, 1995). While the false discovery rate (FDR) method was deployed as a secondary threshold to capture potentially valuable markers missed by Bonferroni correction. FDR threshold was estimated for each model in R with the *qvalue* package version 2.38.0 to retain significant association with <1 false positive (Storey et al., 2024). The adequacy of the models was validated through quantile-quantile (Q–Q) plots to examine the overall distribution of p-values and detect any potential genomic inflation or deflation and by estimating the genomic inflation factor (λ) (Devlin & Roeder, 1999). All models with genomic inflation (λ) below 0.8 or higher than 1.2 were not considered. Q–Q plots and the genomic inflation factor were estimated with the *QQperm* package version 1.0.1 in R (R Core Team, 2024; Wang, 2016). Manhattan plots were generated to visualize the GWAS results, illustrating the $-\log_{10}$ (p-value) for each marker across the seven pea chromosomes, highlighting regions with significant associations. The Manhattan and Q–Q plots were generated with *CMplot* package version 4.5.1 in R (Yin et al., 2021). All markers that could not be mapped to any chromosomes or that mapped on unaligned scaffolds or super-scaffolds were grouped within the arbitrary chromosome 9 on the Manhattan plot for data representation.

2.7 | Candidate gene selection

In the search for potential candidate genes, we examined the genomic regions based on LD (r^2) of 0.2, which placed the ideal genetic distance within 30 kb window. Significant DArTseq markers were then explored for putative genes within this window using the high-resolution pea genome Caméor V1a and the ZW6 reference genome version 1.0 on the pulse crop database website (https://www.pulsedb.org/jbrowses). The gene ontology (GO) annotations of the pea genomes were retrieved from the European Bioinformatics Institute (EMBL-EBI) (Ensembl Genomes at https://plants.ensembl.org, accessed May 18, 2025). Whenever the pea gene could not be linked to any GO terms, we delved into the *A. thaliana* TAIR database (Berardini et al., 2015) to identify corresponding orthologous proteins in this model species.

3 | RESULTS

3.1 | Phenotypic variation of the pea diversity panel to *Fop* race 1

Phenotypic response of the pea diversity panel to *Fop* isolates broadly followed normal distribution for Shapiro–Wilk normality and was confirmed by Pearson normal distribution (Figures 2A and 3A). Results from the three replicated experiments reveal moderate to strong correlation for *Fop* race 1, as demonstrated by the positive and highly significant ($p < 0.001$) Pearson's correlation ranging from 0.38 to 0.72 (Figure 2A). Although moderate skewness and kurtosis were initially detected for the replicated experiments, this was significantly corrected by the estimated BLUPs ($BLUP_{AUDPC}$) of each replicated experiment, with Pearson's correlation coefficient appreciating from 0.69 to 0.86 (Figure 2A). Improvement in the heritability estimates and distribution quality by $BLUP_{AUDPC}$ can be attributed to the

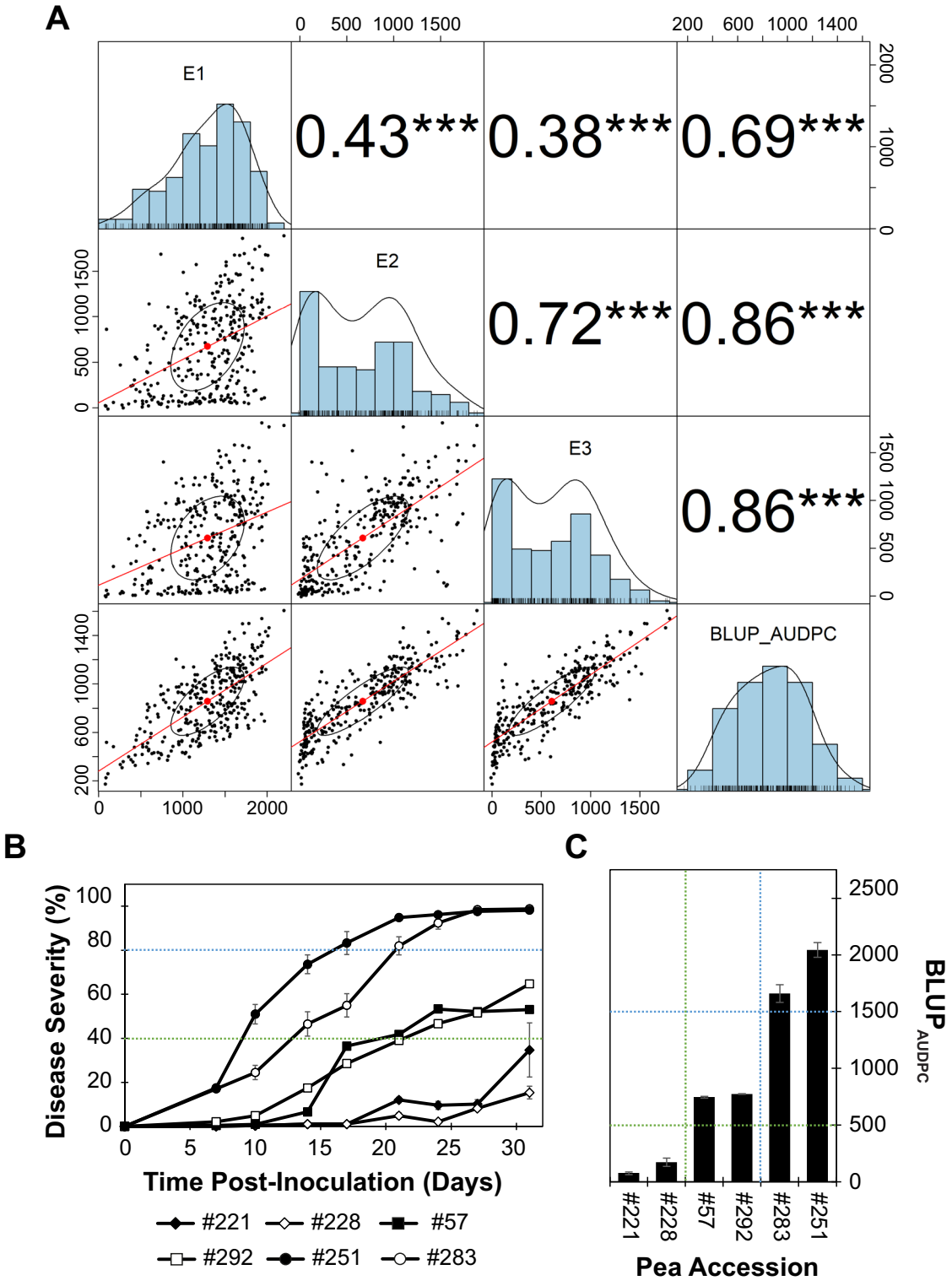

FIGURE 2 Characteristics of the pea response to *Fop* race 1. (A), Distribution of area under disease progress curve (AUDPC) values observed in response to *Fop* race 1 infection for each replicated experiment (E1, E2, and E3) and the estimated $BLUP_{AUDPC}$ (where BLUP is best linear unbiased prediction) dataset (diagonal) and their correlations represented as scatter plots (lower diagonal with red trend line) and as Pearson's correlation coefficient (upper diagonal with significant levels). ***Indicates highly significant correlations at $p < 0.001$. (B), Evolution of disease severity induced by the *Fop* race 1 isolate on selected pea accessions over time, showcasing accessions with intermediate reaction between resistant and susceptible accessions. (C) Histogram comparing the $BLUP_{AUDPC}$ estimates for the selected pea accessions. Blue and green dashed lines represent the limit between the susceptible and intermediate accessions and between the intermediate and resistant accessions, respectively. Error bars represent standard error of the means for $n = 9$.

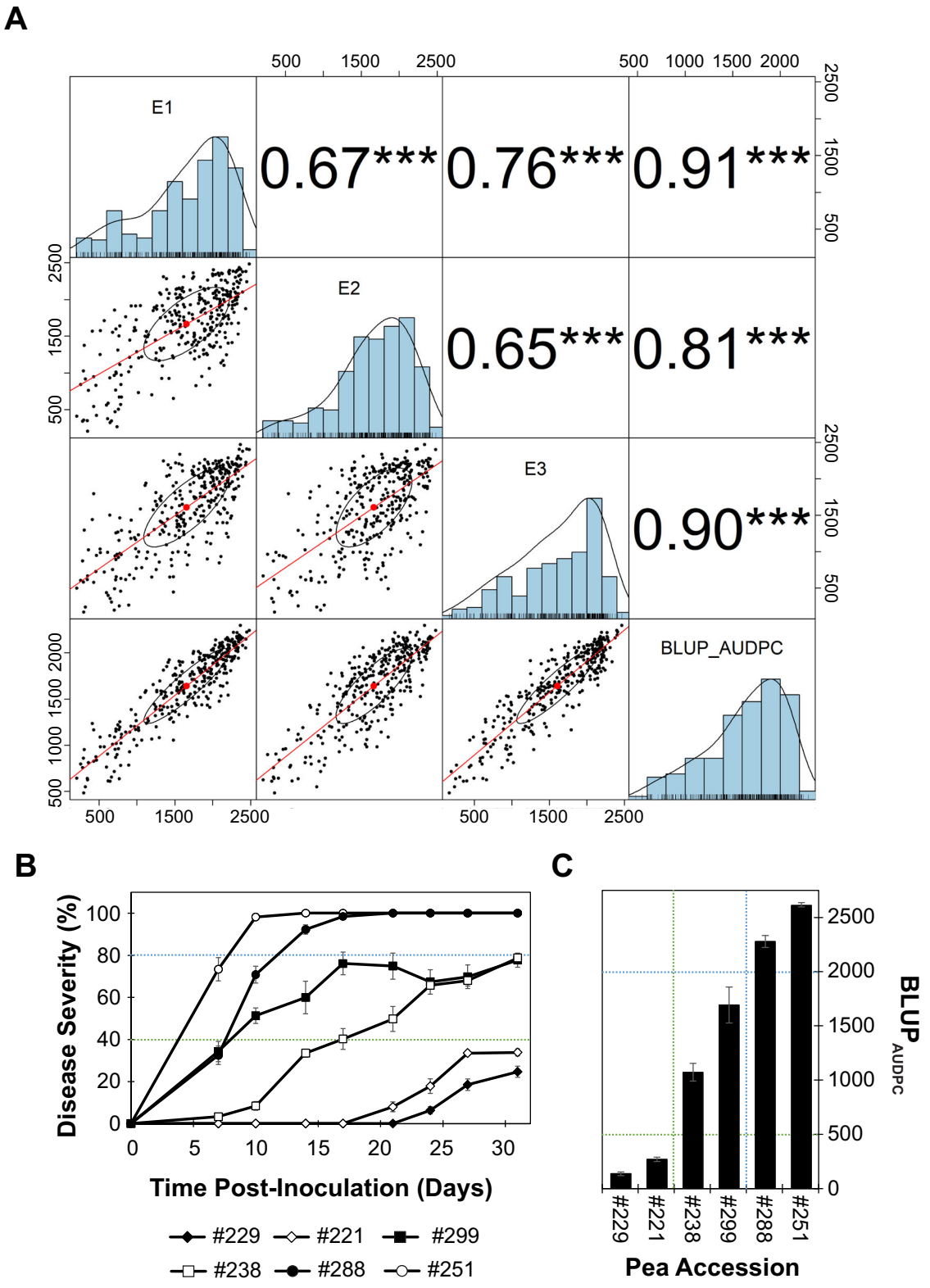

FIGURE 3 Characteristics of the pea response to *Fop* race 2. (A), Distribution of area under disease progress curve (AUDPC) values observed in response to *Fop* race 2 infection for each replicated experiment (E1, E2, and E3) and the estimated $BLUP_{AUDPC}$ (where BLUP is best linear unbiased prediction) dataset (diagonal) and their correlation represented as scatter plots (lower diagonal with red trend line) and as Pearson's correlation coefficient (upper diagonal with significant levels). ***Indicates highly significant correlations at $p < 0.001$. (B) Evolution of disease severity induced by the *Fop* race 2 isolate on selected pea accessions over time clearly evidencing accessions with intermediate reaction between resistant and susceptible accessions. (C), Histogram comparing the $BLUP_{AUDPC}$ estimated for the selected pea accessions. Blue and green dashed lines represent the limit between the susceptible and intermediate accessions and between the intermediate and resistant accessions, respectively. Error bars represent standard error of the mean for $n = 9$.

TABLE 1 Descriptive statistics and heritability.

Fop race	Exp.	Parameter	CV	Maximum	Mean	Minimum	SE	H^2
1	E1	AUDPC	40.9	2299	1290	0	17.1	
1	E2	AUDPC	80.4	2063	669	0	17.5	
1	E3	AUPDC	80.6	2062	601	0	15.7	
1		$BLUP_{AUDPC}$	33	1604	853	172	15.8	0.75
2	E1	AUDPC	40.9	2520	1647	0	21.6	
2	E2	AUDPC	34.4	2520	1667	0	18.4	
2	E3	AUPDC	38.6	2520	1605	0	19.8	
2	Joint	$BLUP_{AUDPC}$	24.7	2295	1640	482	22.5	0.85

Abbreviations: AUDPC, area under disease progress curve; BLUP, best linear unbiased prediction; CV, coefficient of variance; Exp., independent replicated experiments; H^2, broad sense heritability; SE, standard error.

effective removal of environmental and experimental-related variance (Robinson, 1991; Wohor et al., 2025). The pea diversity panel exhibited a high range of phenotypic variations to *Fop* race 1 in terms of their $BLUP_{AUDPC}$ values that ranged from 172 to 1604, reflecting a continuous distribution pattern from resistant to susceptible. A high broad sense heritability (H^2) of 0.75 was observed with 33% of the phenotypic variance explained (PVE) (Table 1).

Welch's ANOVA ($p < 0.001$) confirmed the significant differences observed between accessions in response to this isolate. Pairwise *post hoc* comparison of the $BLUP_{AUDPC}$ values of each pea accession to the most resistant accession #190 (PI 273207) and susceptible accession #251 (PI 505059) revealed three statistically distinct groups (Figure 2B,C; Table S1). Accordingly, 60 accessions were classified as resistant, 194 showed intermediate reactions, and the remaining accessions were classified as susceptible to *Fop* race 1 (Figure 2B,C; Table S1).

3.2 | Phenotypic variation of the pea diversity panel to *Fop* race 2

Large variation was also observed in response to the *Fop* race 2 isolate. Distribution of the phenotypic response to this isolate was continuous but slightly skewed toward susceptibility (Figure 3A). Strong positive and significant ($p < 0.001$) correlations were observed across replicated experiments, ranging from 0.65 to 0.75 for individual replicated experiments. The estimated $BLUP_{AUDPC}$ heightened the significance of each replicated experiment with Pearson's correlation coefficient ranging from 0.81 to 0.91 ($p < 0.001$) (Figure 3A). The broad sense heritability variance (H^2) estimated for *Fop* race 2 resistance was also high in the pea panel, reaching 0.85 (Table 1).

Welch's ANOVA confirmed the large variation observed in the pea diversity panel in response to the *Fop* race 2 isolate ($p < 0.001$). Comparing the $BLUP_{AUDPC}$ of each accession to the most resistant #229 (RADLEY) and susceptible #251 (PI 505059) accessions separated the collection into three groups (resistant, intermediate, and susceptible) (Table S1; Figure S1; Figure 3B,C). Accordingly, 30 accessions were classified as resistant, 97 showed intermediate reactions, and the remaining accessions were susceptible.

3.3 | Response of *Pisum* species and subspecies to *Fop* races 1 and 2

Grouping accessions by species and subspecies revealed large variation ($p < 0.001$) between groups in response to *Fop* (Figure 4; Figure S1). Estimated $BLUP_{AUDPC}$ values observed against *Fop race 1* ranged from 432.4 for *Pisum elatius* var. *elatius* to 1037.3 for the *P. abyssinicum* group, while it ranges from 1506.5 for *P. fulvum* to 2098.4 for *P. abyssinicum* in response to *Fop* race 2 (Figure 4). *Pisum abyssinicum* and the "Indian ecotype" of *P. sativum* presented the highest $BLUP_{AUDPC}$ and appeared as the most susceptible groups in response to both *Fop* isolates (Figure 4). In turn, *P. elatius* and *P. fulvum* accessions showed the lowest $BLUP_{AUDPC}$ values in response to *Fop race 1* and *Fop* race 2, respectively. *Pisum fulvum* also showed moderate resistance to *Fop* race 1. Interestingly, *P.s. sativum* and *P.s. humile* showed moderate resistance to both isolates. Overall, disease severity induced by the *Fop* race 2 isolate was notably higher than that observed in response to the *Fop* race 1 isolate, suggesting a higher virulence of the *Fop* race 2 isolate (McPhee et al., 2012).

3.4 | Population structure of the pea diversity panel

Prior to GWAS, a DAPC analysis was performed to confirm the population structure of the pea panel. Clustering was based on the BIC profile that showed a significant peak at $K = 6$ and confirmed by the automatic selection criteria. Accordingly, six clusters were retained for the DAPC (Figure 5; Figure S2). The first two discriminant axis explained 62.3% of the genetic variance, and the first axis

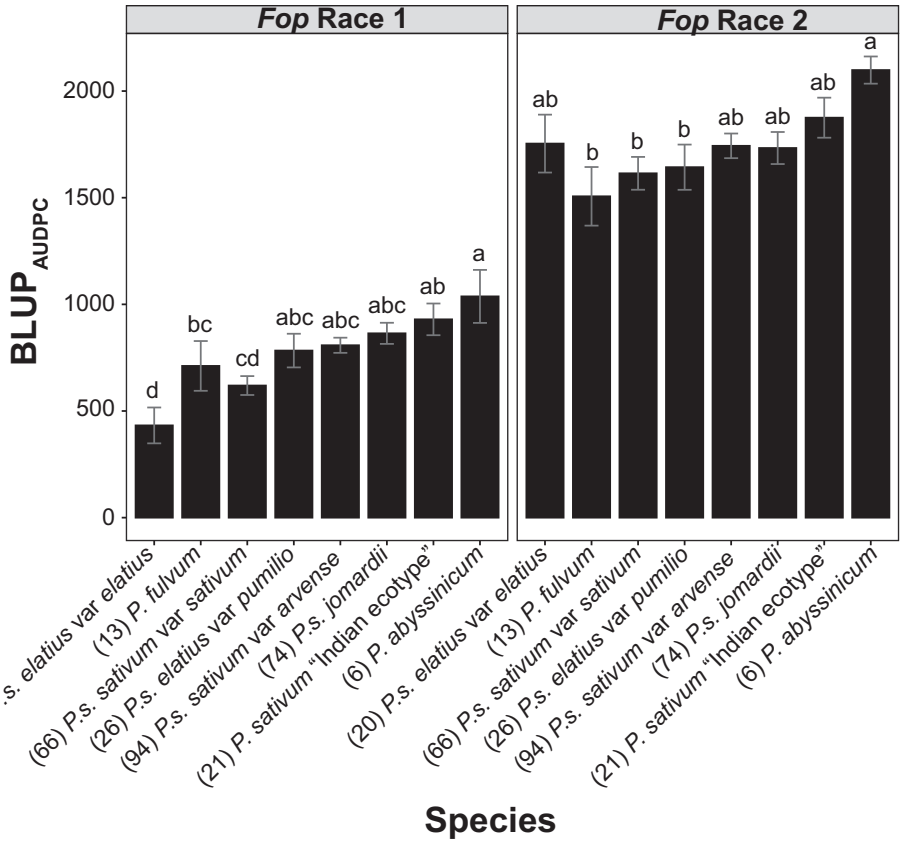

FIGURE 4 Response of *Pisum* species and subspecies to *Fop*. The histograms represent the $BLUP_{AUDPC}$ (where BLUP is best linear unbiased prediction and AUDPC is area under disease progress curve) values observed for each *Pisum* species and *P. sativum* subspecies in response to *Fop* races 1 and 2. Numbers in brackets are the number of accessions. Vertical bars on the histogram represent standard error of difference. For each histogram, different letters indicate statistically significant differences between *Pisum* species and subspecies according to Games-Howell pairwise comparison at $\alpha = 0{,}05$. Error bars represent standard error of the mean.

appears to separate the wild accessions from the landraces. Similar to previous observations (Rispail et al., 2023; Wohor et al., 2025), the DAPC clearly indicated the separation of six clusters. These clusters corresponded to the *P. elatius* var *pumilio* accessions (cluster 1), the *P. fulvum, P. abyssinicum*, and the *P. elatius* var. *elatius* accessions (cluster 2), the "Indian ecotype" of *P. sativum* (cluster 3), the *P.s. sativum* var. *arvense* (cluster 4), the cultivated *P.s. sativum* var *sativum* (cluster 5), and *P.s jomardii* (cluster 6). However, three of the clusters appears to be overlapping—exhibiting highly admixed accessions (clusters 4 and 6) and moderate admixtures (clusters 4 and 5). Similarly, moderate differentiation and admixtures were observed in an earlier study using DAPC (Crosta et al., 2023).

3.5 | MTAs for *Fop* race 1 and 2

To uncover the genetic architecture of *Fop* resistance in pea, a GWAS was conducted using 26,045 SilicoDArT markers with three different models, MLM, BLINK, and FarmCPU. Phenotypic $BLUP_{AUDPC}$ value estimated for each pea accession in response to both *Fop* isolates and the genotypic DArT-marker data were included in the GWAS models. DAPC estimated population structure (Figure 5) differentiated into 6 subgroups with observed admixtures similar to previous studies (Rispail et al., 2023). Thus, population-related covariates (kinship and PCs) were added to each model. The number of informative PCs included in the models was determined according to the scree plot of the genotypic eigenvalues of the PCs plotted against explained variance (Figure S3). This showed that the first three PCs explained the highest variation with the least decay slope and were included as covariates to correct population structure in the GWAS models. Examination of the resulting *Q*–*Q* plots (Figure 6A) showed that the population structure of the pea diversity panel was adequately controlled by the models. This was confirmed by the estimation of the genomic inflation factor (λ) that indicates a well-calibrated range from 0.89 to 1.07. Accordingly, all three models were considered in the analysis.

GWAS results based on the three models identified a total of 15 significant MTAs for *Fop* race 1 resistance (Table 2;

TABLE 2 List of diversity array technology (DArT) markers significantly associated with resistance to *Fop* race 1.

	Marker	Chr[a]	Position[b]	*p* value	MAF	Effect	Model	λ[c]	LOD[d]	PVE[e]
1	3551059	3LG5	69,902,518	5.79E-09	0.19	99.37	BLINK	0.95	8.84	24.74
				7.42E-08		87.47	FarmCPU	0.89	7.13	19.17
2	3560253	3LG5	110,942,273	1.28E-06	0.26	86.68	BLINK	0.95	6.67	26.00
3	5949840	3LG5	432,495,164	3.70E-07	0.07	157.01	BLINK	0.95	7.13	23.03
4	3641226	4LG4	1,025,162	2.57E-05	0.05	−124.25	FarmCPU	0.89	5.49	10.82
5	5900892	4LG4	147,449,609	2.00E-05	0.08	82.99	FarmCPU	0.89	5.49	7.02
6	4654955	5LG3	22,448,528	1.03E-05	0.11	−108.41	FarmCPU	0.89	5.65	17.47
7	3544927	5LG3	119,138,446	2.41E-05	0.10	106.37	FarmCPU	0.89	5.49	14.41
8	3552330	5LG3	284,688,721	2.32E-11	0.36	86.08	BLINK	0.95	10.94	36.03
				8.10E-07		56.14	FarmCPU	0.89	6.57	15.33
9	3548203	5LG3	491,740,484	1.12E-05	0.41	51.37	FarmCPU	0.89	5.65	14.46
10	5929725	6LG2	13,287,647	1.61E-11	0.23	−106.23	BLINK	0.95	10.94	34.02
				4.29E-07		−74.01	FarmCPU	0.89	6.67	16.52
11	5931038	Unknown		5.80E-05	0.18	−126.53	MLM	1.03	4.65	39.09
12	5964436	Unknown		4.62E-11	0.06	−178.67	BLINK	0.95	10.81	25.08

[a]Chromosome nomenclature based on the Caméor v1a reference genome.
[b]Location of the DArT marker onto the Caméor v1a reference genome.
[c]Genomic inflation factor (λ).
[d]logarithm of the odds value estimated as the $-\log_{10}(p \text{ value})$.
[e]Percentage of phenotypic variance explained by the marker in the genome-wide association study (GWAS) model.
Abbreviations: BLINK, Bayesian information and Linkage-disequilibrium Iteratively Nested Keyway; MAF, minor allele frequency; MLM, mixed linear model.

Figure 6B). The highest number of significant MTA was uncovered by FarmCPU (eight MTAs), closely followed by BLINK (six MTAs), while MLM only detected one significant MTA (Table 2). Two of the informative markers located on chromosome 3 (3,551,059) and chromosome 5 (3,552,330) were captured by both BLINK and FarmCPU models (Table 2). Significant MTAs are explained from 10.82 to 39.09 of the phenotypic variances. They corresponded to 12 individual markers scattered on four pea chromosomes (Table 2). The highest number of significant MTAs were found on chromosome 5 with 4 significant MTAs, closely followed by chromosome 3 with 3 MTAs, chromosome 4 with 2 MTAs, and chromosome 6 with 1 MTA. Two additional MTAs could not be mapped onto any of the pea chromosomes.

For resistance to the race 2 isolate, a total of 27 significant MTAs were detected. Four of them were detected by at least two models (Figure 6; Table 3). The BLINK and FarmCPU models captured the highest number of significant MTAs with 13 and 12 MTAs, respectively, while MLM solely detected 2 MTAs. Interestingly, marker 3553942 located on chromosome 4 was identified by all models. BLINK and FarmCPU also identified associated markers 3547272 and 3542143 on chromosome 3 (Table 3). The significant MTAs explained from 12.49 to 92.43% of the phenotypic variances and mapped onto four of the seven pea chromosomes. Chromosome 2 contained the highest number of significant MTAs (7 MTAs), followed by chromosome 4 (6 MTAs), chromosome 3 (4 MTAs), chromosome 1 (2 MTAs), and chromosome 5 (1 MTA), while two additional MTAs could not be mapped. None of the markers detected for *Fop* race 2 resistance were associated with *Fop* race 1 resistance, and no overlaps were detected between these analyses, confirming that the genetic bases of resistance to these two *Fop* races are distinct.

Comparison of associated marker positions with previously reported QTLs revealed that marker 3552330, associated with resistance to *Fop* race 1, co-localizes with the confidence interval (CI) of the *Fw* QTL on Chr5LG3. Likewise, three DArT markers—3569901, 3553942, and 5927288—were located within the CI of the major *Fop* race 2 *Fnw4.1* QTL on Chr4LG4. Additionally, markers 3568469 and 3544927 fell within the CI of *Fnw3.1* on Chr5LG3. Notably, marker 5929725 was positioned within the CI of a QTL associated with *Fop* race 5 *FwS1* QTL on Chr6LG2. Location of previously identified QTLs on the pea genetic map are based on the integration of found loci with published information (Deng et al., 2024; Jain et al., 2015; McPhee et al., 2012) and the position of the surrounding markers available in the Pulse Crop database (https://www.pulsedb.org) (Figure 7).

3.6 | Putative candidate genes for resistance to *Fop* race 1 and 2

To identify potential candidate genes, the genomic region surrounding the significant MTAs was examined within a

TABLE 3 List of diversity array technology (DArT) markers significantly associated with *Fop* race 2 resistance.

	Marker	Chr[a]	Position[b]	*p* value	MAF	Effect	Model	λ[c]	LOD[d]	PVE[e]
1	3544513	1LG6	280,563,070	2.21E-05	0.09	−111.16	BLINK	1.07	5.78	12.49
2	5942042	1LG6	343,080,828	2.12E-05	0.29	−131.20	BLINK	1.07	5.78	58.86
3	3565825	2LG1	506,394	7.59E-07	0.16	−101.38	FarmCPU	1.04	6.80	19.65
4	3557785	2LG1	92,608,135	1.57E-07	0.33	126.00	FarmCPU	1.04	7.11	62.17
5	3642316	2LG1	293,350,085	1.07E-08	0.17	140.63	BLINK	1.07	8.46	39.63
6	3542638	2LG1	311,379,473	1.63E-05	0.32	84.52	FarmCPU	1.04	5.75	26.79
7	5921966	2LG1	337,317,411	3.74E-05	0.48	71.80	FarmCPU	1.04	5.51	29.19
8	8054390	2LG1	356,856,867	1.96E-05	0.21	−86.04	FarmCPU	1.04	5.75	17.97
9	3566463	2LG1	375,161,010	3.80E-07	0.14	129.79	BLINK	1.07	7.13	27.87
10	3547272	3LG5	82,185,090	1.21E-06	0.49	−76.58	FarmCPU	1.04	6.77	33.85
				2.13E-06		−84.60	BLINK	1.07	6.53	41.32
11	4659845	3LG5	106,406,021	1.01E-06	0.10	156.46	FarmCPU	1.04	6.78	28.80
12	100000325	3LG5	139,624,472	1.79E-05	0.08	117.82	FarmCPU	1.04	5.75	12.50
13	3542143	3LG5	301,200,334	9.97E-07	0.36	−121.37	BLINK	1.07	6.79	62.56
				1.38E-06		−107.48	FarmCPU	1.04	6.77	49.06
14	5965595	4LG4	*87,212,774*	5.07E-07	0.18	118.23	FarmCPU	1.04	6.80	29.81
15	44298773	4LG4	277,838,697	7.96E-07	0.11	145.38	FarmCPU	1.04	6.80	26.81
16	3569901	4LG4	303,104,597	4.96E-06	0.28	82.40	BLINK	1.07	6.32	22.47
				1.59E-05		130.80	MLM	0.99	5.10	56.61
17	3553942	4LG4	307,746,285	2.25E-17	0.21	192.98	BLINK	1.07	16.66	92.43
				6.92E-09		115.08	FarmCPU	1.04	8.16	32.87
				2.79E-07		173.54	MLM	0.99	6.56	74.74
18	5927288	4LG4	322,783,867	1.95E-07	0.25	105.54	BLINK	1.07	7.33	32.56
19	5935763	4LG4	395,679,088	5.58E-09	0.11	−163.58	BLINK	1.07	8.57	35.42
20	3568469	5LG3	102,251,688	4.23E-06	0.25	−97.75	BLINK	1.07	6.32	28.28
21	35620800	Unknown		4.93E-06	0.15	−118.68	BLINK	1.07	6.32	25.38
22	5958608	Unknown		1.57E-05	0.07	−132.19	BLINK	1.07	5.86	14.13

[a]Chromosome nomenclature based on the Caméor v1a reference genome.
[b]Location of the DArT marker onto the Caméor v1a reference genome.
[c]Genomic inflation factor (λ).
[d]logarithm of the odds value estimated as the $-\log_{10}(p \text{ value})$.
[e]Percentage of phenotypic variance explained by the marker in the genome-wide association study (GWAS) model.
Abbreviations: MAF, minor allele frequency; MLM, mixed linear model

window of 30 kb on the Caméor V1a and ZW6 genomes. This approach elucidated 28 putative genes, of which 9 genes were linked to *Fop* race 1 resistance, and 19 genes to *Fop* race 2 resistance (Table 4).

The criteria for selecting candidate genes were based on effective MTAs captured by multiple models, high logarithm of the odds scores, and high PVEs as reflected in the most significant MTAs (Tables 2 and 3). Suitably, Chr3 and Chr5 represented MTA hotspots for *Fop* 1, while hotspots for *Fop* 2 were centered on Chr2 and Chr4 (Figures 6 and 7; Table 4). Genes identified close to associated markers were considered the key contributors to *Fop* resistance. Accordingly, four putative genes were identified as candidate genes for *Fop* race 1 resistance (Table 4). These include a putative homolog of FERONIA receptor-like kinase (*Psat3g204560*), containing the marker 3551059 on chromosome 3; an adenosine triphosphate (ADP/ATP carrier protein (*Psat4g001520*) that contain the marker 3641226 on chromosome 4; a reverse transcriptase (*Psat5g156040*) located 0.03 kb downstream of marker 3552330 on Chr5LG3, and an Exo70 exocyst complex subunit-like protein (*Psat6g017800*) on Chr6LG2 that contains the marker 5929725.

Subsequently, seven putative genes were identified close or in the vicinity of the markers associated with *Fop* race 2 resistance (Table 4). This included an alpha-beta hydrolase (*Psat1g140520*) located on chromosome 1 that contains the marker 3544513; a conserved oligomeric complex COG6-like protein (*Psat2g146720*) on chromosome

TABLE 4 Annotation of the closest candidate genes surrounding the diversity array technology (DArT) markers associated with Fop resistance.

Marker	Distance (kb)	Gene ID	Gene annotation	GO term		InterPro	
				ID	Description	ID	Description
Resistance to *Fop* race 1							
3560253	in	*Psat3g051960*	PfkB family carbohydrate kinase	0061594	6-Deoxy-6-sulfofructose kinase activity	IPR002139	Ribo/fructo_kinase
5949840	−5.5	*Psat3g204560*	Receptor-like protein kinase FERONIA-like	0004674 0004717	Protein Ser/Thr kinase activity Transmembrane receptor protein tyrosine kinase activity	IPR045272	Receptor-like protein kinase ANXUR1/2-like
3551059	in	*Psat0s425g0040*	Hypothetical protein				
3641226	in	*Psat4g001520*	ADP/ATP carrier protein ER-ANT1 like	0140021 1990544	Mitochondrial ADP transmembrane transport Mitochondrial ATP transmembrane transport	IPR002113 IPR002067	ADP/ATP carrier protein, eukaryotic type Mitochondrial carrier protein
5900892	3.9	*Psat4g084560*	F-box protein SKIP2 like	0031146 0005515	SCF-dependent proteasomal ubiquitin-dependent protein catabolic process Protein binding	IPR001810 IPR032675	F-box domain Leucine-rich repeat domain superfamily
4654955	in	*Psat5g013120*	Gibberellin regulated protein	0009739	Response to Gibberellin	IPR003854	GASA
3548203	in	*Psat5g246000*	Unknown protein	*At3g15518*[a]			
3552330	0.03	*Psat5g156040*	Reverse transcriptase	0003824	Catalytic activity	IPR000477 IPR043502	Reverse transcriptase domain DNA/RNA polymerase superfamily
5929725	in	*Psat6g017800*	Exo70I exocyst complex subunit	0006887 0005546	Exocytosis Phosphatidylinositol-4,5-bisphosphate binding	IPR004140	Exocyst complex component Exo70
Resistance to *Fop* race 2							
3544513	In	*Psat1g140520*	Alpha/beta-Hydrolases superfamily	*At3g47560*[a]	Stress response (drought, salinity, or pathogen attack)[a]	IPR029058	Alpha/Beta hydrolase fold
5942042	in	*Psat1g191560*	Plastid transcriptionally active 12 like protein	0045893 0042793 0090228	Positive regulation of DNA-templated transcription Plastid transcription Positive regulation of red or far-red light signalling pathway	IPR034581	PTAC12
3642316	in	*Psat2g112360*	Hypothetical protein				

(Continues)

TABLE 4 (Continued)

Marker	Distance (kb)	Gene ID	Gene annotation	GO term ID	GO term Description	InterPro ID	InterPro Description
5921966	in	*Psat2g130280*	Ureide permease 2 like	0071705	Nitrogen compound transport	IPR030189	Ureide permease, plant
				0005274	Allantoin:proton symported activity		
				0015505	Uracyl: monoatomic cation symported activity		
3566463	in	*Psat2g146720*	Conserved oligomeric complex COG6	0006891	Intra-Golgi vesicle-mediated transport	IPR010490	Conserved oligomeric Golgi complex subunit 6
3542638	−2.3	*Psat2g119600*	Cation/(H+) antiporter 14-like	0006885	Regulation of pH	IPR050794	Monovalent cation:proton antiporter 2
				1902600	Proton transmembrane transport	IPR038770	Sodium/solute symporter superfamily
				0015297	Antiporter activity	IPR006153	Cation/H+ exchanger
3,565,825	−12.2	*Psat2g000680*	Homoserine kinase	0009088	Threonine biosynthetic process	IPR000870	Homoserine_kinase
				0004413	Homoserine kinase activity		
8054390	−12.6	*Psat2g137320*	Transcription factor MYB41-like	0003700[a]	DNA-binding transcription factor activity[a]	IPR015495	Myb transcription factor, plants
3547272	in	*Psat3g037400*	Sulfite exporter TauE/SafE	0016567	Protein ubiquitination	IPR002781	Transmembrane protein TauE-like
4659845	in	*Psat3g049760*	Hsp70 protein	0006397	mRNA processing	IPR013126	Heat shock protein 70 family
				0140662	ATP-dependent protein folding chaperone		
100000325	in	*Psat3g066240*	RNA Demethylase AlkBH10B-like	0006422	mRNA catabolic process	IPR044842	RNA demethylase ALKBH9B/ALKBH10B-like
				0032451	Demethylase activity		
3542143	in	*Psat3g156440*	Phosphoglycerate mutase family protein	0003824	Catalytic activity	IPR012398	PRIB5
						IPR013078	Histidine phosphatase superfamily, clade-1
44298773	in	*Psat4g140960*	RNI-like superfamily protein	0035556	Intracellular signal transduction	IPR052201	Leucine-rich repeat-containing regulator of pluripotency
3569901	in	*Psat4g155360*	Hypothetical protein				
5935763	in	*Psat4g192760*	WAS/WASL -interacting family	*At1g55160*[a]			
5965595	−1.4	*Psat0s4095g0040*	Zinc finger CCCH domain-containing protein 39 like	0006355	Regulation of DNA-templated transcription	IPR045877	RNA-binding protein ZFP36-like

(Continues)

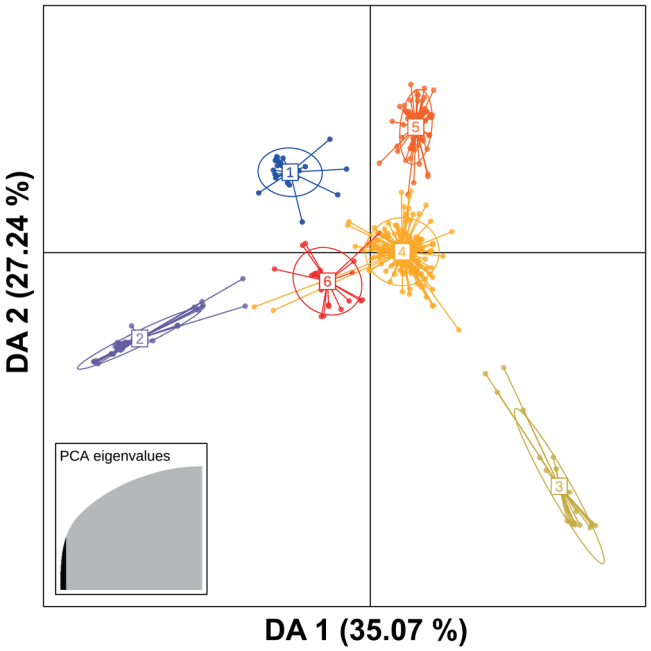

FIGURE 5 Genetic structure of the pea diversity panel. The scatterplot shows 6 distinct clusters of the first two discriminant axis of the discriminant analysis of principal components (DAPC). Cluster 1 contains all *Pisum elatius* var *pumilio*; cluster 2 regroups the accessions from *Pisum fulvum*, *P. elatius* var. *elatius* and *Pisum abyssinicum*; cluster 3 contains the accession of the "Indian ecotype" of *Pisum sativum*; cluster 4 contains the *P.s. sativum* var. *arvense* accessions; cluster 5 the cultivated *P.s. sativum* var *sativum;* cluster 6 contains the accessions from *P.s. jomardii*. The first axis separates wild versus landrace material, while admixtures are observed among clusters 4, 6, and 4, 5.

TABLE 4 (Continued)

Marker	Distance (kb)	Gene ID	Gene annotation	GO term		InterPro	
				ID	Description	ID	Description
3553942	−5.2	*Psat4g157160*	Glycosyl transferases group 1	0016757	Glycosyltransferase activity	IPR001296	Glycosyl transferase, family 1
5927288	24.8	*Psat4g166640*	Trihelix transcription factor ASIL2 like	0000976	Transcription cis-regulatory region binding	IPR044823	ASIL1/2-like
3568469	in	*Psat5g056120*	Calcium-dependent mitochondrial ATP-magnesium/phosphate carrier protein 5 like	0015866 0015867	ADP transport ATP transport	IPR002067 IPR002048	Mitochondrial carrier protein EF-hand domain

Note: These genes were annotated on the pea Caméor V1a reference genome. "in" the marker sequence is located within the gene sequence.
Abbreviations: ATP, adenosine triphosphate; GO, gene ontology.
[a]The closest Arabidopsis thaliana homologs.

2 that contain the marker 3566463; a sulfite exporter TauE/SafE (*Psat3g037400*); and a phosphoglycerate mutase family protein (*Psat3g156440*), both located on chromosome 3 and containing the markers 3547272 and 3542143, respectively. It also included a group 1 glycosyl transferase-like protein (*Psat4g157160*) located 5.19 kb upstream of marker 3553942 and calcium-dependent mitochondrial ATP-magnesium/phosphate carrier protein (*Psat5g056120*) on Chr5LG3 containing the marker 3568469 and several transcription factors. These candidate genes have been associated with root detoxification processes, stress responses, and defense functions that are key in plant immunity. Accordingly, they might be implicated in *Fop* resistance in pea.

4 | DISCUSSIONS

FW is one of the major constraints of pea worldwide (Verma et al., 2025). Earlier screenings for resistance have identified some resistant accessions that were efficiently transferred to pea elite cultivars (Wohor et al., 2022). However, exist-

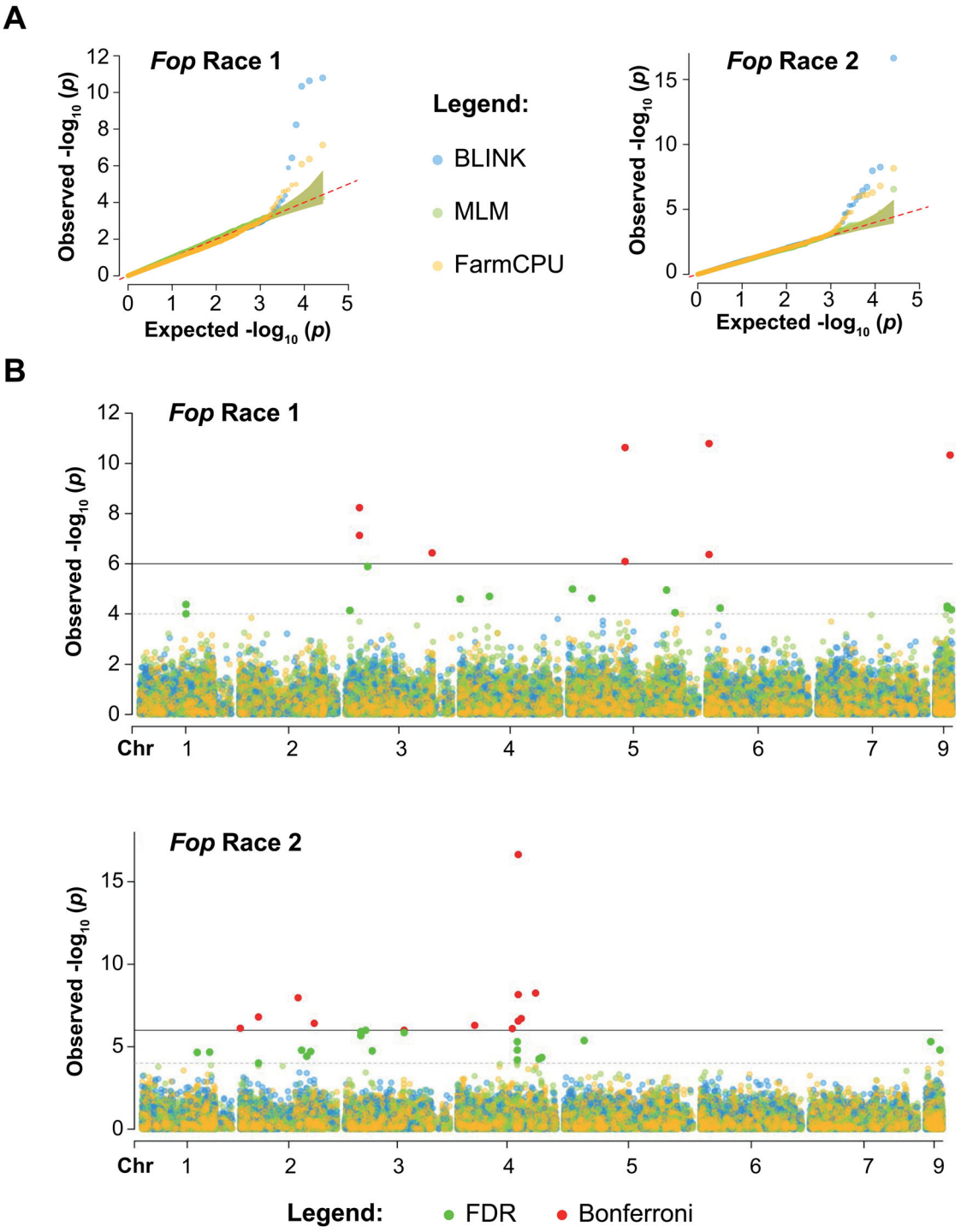

FIGURE 6 Superposed *Q*--*Q* plots (A) and Manhattan plots (B) of the genome-wide association study (GWAS) model outputs for *Fop* race 1 and 2 resistance. Arbitrary chromosome 9 represents unmapped markers. In the Manhattan plots, red and green dots show markers significantly linked to *Fop* resistance within the Bonferroni and false discovery rate (FDR) thresholds. The black solid and grey dotted lines indicate the logarithm of the odds (LOD) estimated thresholds for Bonferroni and FDR, respectively. BLINK, Bayesian information and linkage-disequilibrium iteratively nested keyway; FarmCPU, fixed and random model circulating probability unification; MLM, mixed linear model.

ing resistance breeding strategies mainly rely on monogenic mechanisms that are vulnerable to *Fop* pathogen adaptation (Infantino et al., 2006). Despite its importance, only a few studies have investigated the genetic basis of *Fop* resistance, and the identification of *Fop* resistance genes remains elusive. Resistance to races 1 and 5 was shown to be influenced by single race-specific genes (*Fw*, *Fwf*, and *FwS1*) found on Chr5LG3 and Chr6LG2, respectively (Coyne et al., 2000;

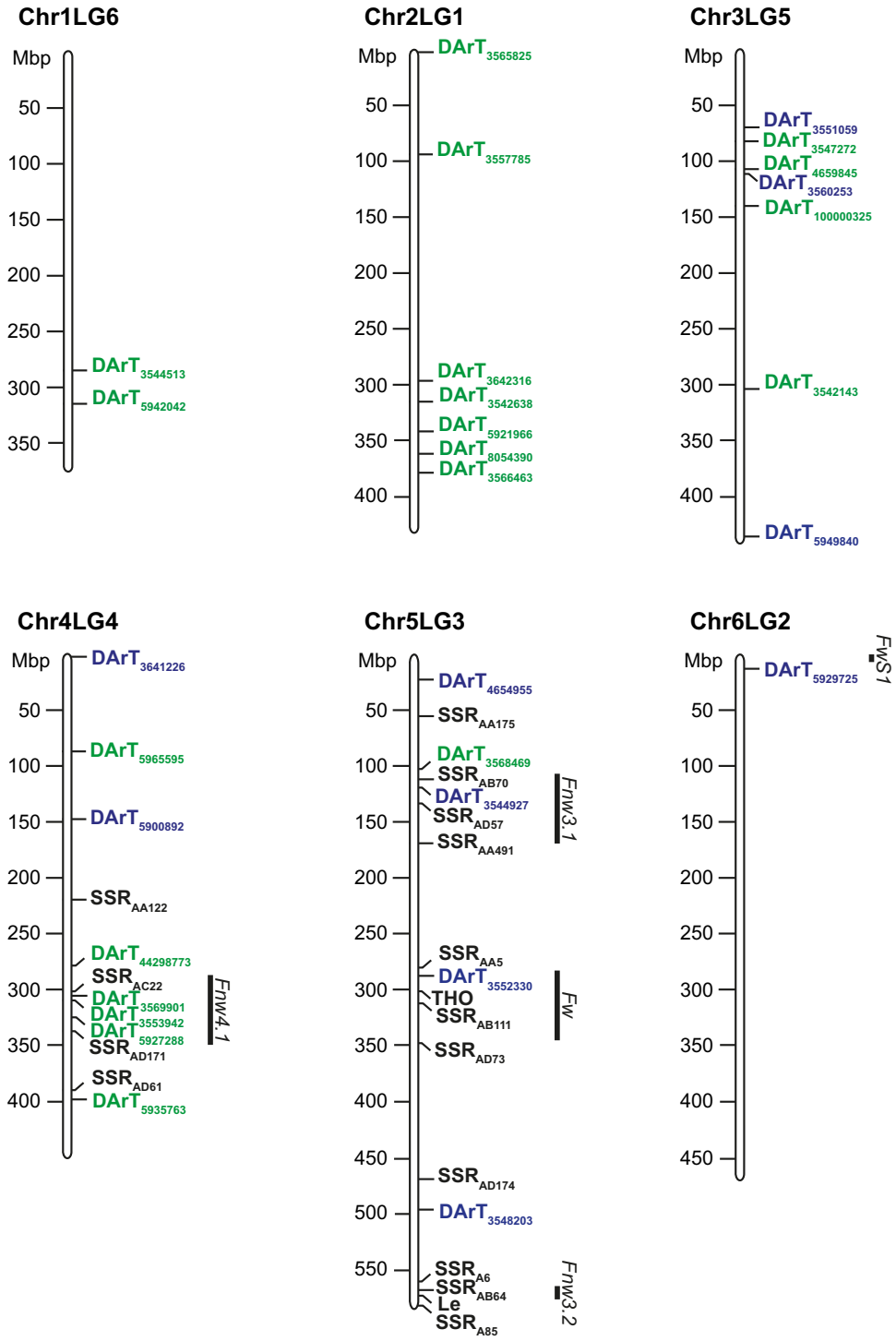

FIGURE 7 Location of significant marker-trait associations (MTAs) and previous QTL for resistance to *Fop* on pea genetic map. The figure shows the location of the diversity arrays technology sequencing (DArTSeq) markers (in bold) associated with resistance to *Fop* race 1 (blue), *Fop* race 2 (green), and previously identified quantitative trait locus (QTL) (boldly underlined) for *Fop* resistance on a schematic representation of the pea chromosomes and linkage groups.

Deng et al., 2024; Jain et al., 2015). In contrast, resistance to race 2 was quantitative and influenced by at least three loci (*Fnw3.1*, *Fnw3.2*, and *Fnw4.1*) on Chr4LG4 and Chr5LG3 (Bani et al., 2012; McPhee et al., 2012). Although markers have been proposed for the selection of resistant lines to *Fop* races 1 and 2 (Jain et al., 2015; McPee et al., 2012), the large genetic distance between markers and resistance loci hinders MAS implementation. Success of breeding programs is determined by the availability of diverse genetic pools with substantial genetic variation (Pandey et al., 2021). Thus, there

is the need to broaden the genetic diversity of pea to improve *Fop* resistance durability and further characterize the resistance loci for easier transfer to elite cultivars. To this aim, this study evaluated the response of a wide pea diversity panel to *Fop* races 1 and 2 and identified novel molecular markers and candidate genes associated with resistance to *Fop* (Table 4).

Phenotypic assessment of *Fop* was carried out with 324 diverse pea panel under controlled conditions in growth chambers, following ideal pea growth conditions. Although controlled experiments are mostly designed without blocking, a factorial design in RCBD was deployed here to eliminate potential microclimatic variations. Findings revealed a wide range of responses to both *Fop* races (Figures 2 and 3). Contrary to previous reports suggesting the strictly qualitative inheritance pattern of *Fop* race 1 resistance (Jain et al., 2015; McClendon et al., 2002), our study identified a quantitative response to this race similar to the resistance detected in *Fop* race 2 (Bani et al., 2012). This knowledge could be instrumental in complementing R-gene-mediated resistance and improving durability of *Fop* resistance in the field (Rubiales et al., 2023). As previously detected in grass pea (Sampaio et al., 2021), we found that *Fop* resistance in pea is under strong genetic control as indicated by the high heritability estimates of both races (Table 1), which would facilitate early-stage selection of resistant lines (Piepho & Moehring, 2007).

This study confirmed the resistant phenotype of accessions #221 (JI 1412), #222 (JI 1559), #229 (Radley), #280 (IFPI 3365), #290 (IFPI 2356), and #291 (IFPI 2357) to *Fop* race 2 (Bani et al., 2012; Neumann & Xue, 2003). More importantly, the findings uncover novel resistance sources with high level of resistance, adding to the previously detected resistance sources (Bani et al., 2012; Deng et al., 2022; McPhee et al., 1999). Interestingly, some accessions showed resistance to both races while others were specific to a single race (Table S1), which presents a valuable opportunity to investigate the genetic basis of resistance. While several *P.s. sativum* var *sativum* lines exhibited varying levels of *Fop* resistance, wild *P. fulvum* and *P. elatius* var. *elatius* consistently demonstrated superior resistance (Figure 4). This further underscores the usefulness of wild relative as reservoir of novel disease resistance genes for crop improvement (Rubiales et al., 2023).

Given the potential impact of population structure and LD on association mapping (Myles & Wayne, 2008), the DAPC differentiation of the population into six groups was consistent with earlier studies (Rispail et al., 2023; Wohor et al., 2025). Thus, depicting a strong distinctive, genetic makeup—validating the panel's usefulness in GWAS. DAPC observed genetic differentiation relative to MTAs could be considered valuable for optimizing untapped genetic variation discovery in association and genetic selection studies (Crosta et al., 2023). Moderate LD decay demonstrated here was also valuable for enhancing the statistical power of detected variants in GWAS models and accelerated the identification of valuable genes (Gali, Sackville, et al., 2019; Myles & Wayne, 2008). For traits with moderate to high heritability, as in our study, phenotypic BLUPs combined with mixed-GWAS models are reported to consistently produce robust associations while effectively minimizing spurious signals (Robinson, 1991; Wohor et al., 2025).

The implementation of a single locus (MLM) and two multi-locus GWAS models (BLINK and FarmCPU) were efficient in uncovering 42 significant MTAs for *Fop* resistance, of which 15 MTAs represent resistance to race 1 and 27 MTAs for race 2. FarmCPU and BLINK models detected the highest number of MTAs, reflecting their reported superior efficiency (Wang et al., 2022). Hence, justifying the adequacy of the Scree plot enabled inclusion of three PCs (Figure S3) in the GWAS models. Detected MTAs explained between 12.49% and 92.43% of the phenotypic variance and were mapped onto six of the seven pea chromosomes. This wide MTA coverage supports the polygenic and quantitative nature of *Fop* resistance (Tables 3 and 4; Figure 7). In addition, no overlap was detected between the loci associated with resistance to *Fop* races 1 and 2, confirming that the genetic makeup of resistance is race-specific (Deng et al., 2022; Jain et al., 2015; McPee et al., 1999). On the other hand, several markers fell within the CI of four previously detected *Fop* resistance QTL (Jain et al., 2015; McPee et al., 2012), confirming these QTLs and refining their location. In particular, three markers (3569901, 3553942, and 5927288) explaining about 32.56%–92.43% of the variance co-localized with the major *Fop* race 2 resistance QTL *Fnw4.1*, providing a more precise location of this locus on chromosome 4 (Figure 7; Table 4) (McPhee et al., 2012). Moreover, our study uncovers novel genomic regions associated with *Fop* resistance (Figure 7) that would be useful for breeding durable resistance and as a foundation for functional genetic analysis of *Fop* resistance in pea. Out of the 42 significant MTAs, 34 could be mapped to specific regions of the pea genome, allowing the detection of 28 candidate genes that are associated with *Fop* resistance in pea. This demonstrates that the 30 kb window was adequate for detecting annotated genes (as extention to 100 kb did not detect additional MTAs). Accordingly, these putative genes involve several molecular pathways, including regulation of transcription, cell signaling, intracellular vesicle trafficking, and defense (Table 4).

For *Fop* race 1 resistance, four putative genes emerged as key resistance candidates: *Psat5g156040*, *Psat6g017800*, *Psat4g001520*, and *Psat3g204560*. Notably, *Psat5g156040*, encoding a reverse transcriptase, was detected at 0.03 kb upstream of marker 3552330 within the CI of the *Fw* resistance loci (Jain et al., 2015). Besides refining the locus of *Fw*, this locus links *Fop* resistance to retrotransposon activity, although further studies would be needed to confirm

this hypothesis. The second gene, Psat6g017800, encodes an Exo70I-like gene. Exo70 subunits are key members of the exocyst complex that mediate tethering of vesicle to the plasma membrane (De la Concepcion, 2023). Previous studies on the Psat6g017800 ortholog in *Medicago truncatula* demonstrated that EX70I plays a key function during arbuscular mycorrhiza symbiotic interaction (Zhang et al., 2015), which points to a relation between symbiosis and soilborne pathogen infection. Moreover, several EXO70 paralogs in Arabidopsis and wheat have been reported to be involved in plant defenses. For example, EXO70 was found to play key roles in papilla formation during cell wall reinforcement and linked with the powdery mildew susceptibility MLO genes (De la Concepcion, 2023; Huebbers et al., 2024). Similarly, papilla establishment was previously detected in *Fop*-resistant pea root (Bani et al., 2018), implying that EXO70 genes could play a role in delaying *Fop* mycelia growth to enforce resistance. The gene, *Psat4g001520*, encodes for an ADP/ATP carrier-like protein and is orthologous to ER-ANT1. This acyl carrier protein play a key role in plant cells, providing energy for organelle and plastid function—making them crucial for plant growth, development, and environmental adaptation (Nunes-Nesi et al., 2020). In Arabidopsis, ER-ANT1 has been shown to be required for photorespiration and the control of reactive oxygen species generation, which might play a resistance function, albeit its relation with defense is currently unknown (Hoffmann et al., 2013). Finally, *Psat3g204560* encodes a FERONIA-like receptor kinase. These FERONIA and FERONIA-related receptor kinase (FER-RK) have been extensively studied and found to be required for many biological processes in plants, ranging from fertility to immunity (Cheung, 2024). In relation to plant immunity, research has identified FER-RK as a pathway regulating both pattern-triggered immunity and effector-triggered immunity (Ortiz-Morea et al., 2022). Particularly, it was found to be the target for specific pathogen effector of *F. oxysporum* in Arabidopsis (Masachis et al., 2016). This suggests that *Psat3g204560* could play a role in *Fop* resistance but requires further validation.

On the other hand, seven candidate genes were detected near the most relevant markers associated with *Fop* race 2 resistance (Table 4). These genes include a glycosyltransferase group 1-like protein (*Psat4g157160*) and an ASIL-2 trihelix-like transcription factor (*Psat4g166640*), both located within the CI of the *Fnw4*.1 locus (McPhee et al., 2012). Glycosyl transferase and tri-helix transcription factors are noted to be involved in many biological processes responsible for plant´s response to biotic and abiotic stresses (Lao et al., 2014; X. Liu et al., 2020), although their functions in pea need further studies. Three additional transcription factors were also identified near *Fop* race 2 resistance-associated markers, including a putative zinc-finger CCCH type (*Psat0s4095g0040*), a myeloblastosis domain containing transcription factor (*Psat2g137320*), and a plastid transcriptionally active protein-12 ortholog (*Psat1g191560*). Homologs of these transcription factors have been involved in the regulation of different processes to mediate plant adaptation to stresses (Bogamuwa & Jang, 2014; Chen et al., 2010; Yanhui et al., 2006). In particular, their closest orthologs in Arabidopsis and tomato were shown to mediate tolerance to various abiotic stresses such as photomorphogenesis and thermos-morphogenesis (Lashbrooke et al., 2016; Qiu et al., 2015; Xu et al., 2023). Moreover, a zinc finger was found to encode a regulator of hypocotyl elongation and associated with the soybean domestication gene *ZmZFP1*–a key protein involved in plant adaptation (Li et al., 2026). This might also illustrate the interplay between adaptation to abiotic stresses and resistance to FW. Apart from these transcription factors, a conserved oligomeric Golgi complex (COG) 6 homologs for the gene *Psat2g146720* was also detected. Recent studies have highlighted the role of the COG complex in plant-pathogen interactions. In legumes, members of COG have been implicated in defense against fungal pathogens and plant-parasitic nematodes, contributing to the plant's ability to mount an effective immune response (Klink et al., 2022). A sulfite exporter, TauE/SafE (*Psat3g037400*), and a phosphoglycerate mutase (*Psat3g156440*) were also implicated in *Fop* resistance. These histidine proteins are essential for regulating sulfur metabolism, facilitating detoxification processes, and modulating the signaling pathways that enable the plant to adapt and resist pathogens (Rigden, 2019). In addition, a homoserine kinase (*Psat2g000680*) and an Hsp70 homolog (*Psat3g049760*, where Hsp is heat shock protein) have been detected near minor MTAs (Table 4). Previous study on their closest orthologs in several species signals their involvement in plant defense against pathogens, making them strong candidates for further studies into *Fop* resistance (Berka et al., 2022; van Damme et al., 2009). A calcium-dependent mitochondrial ATP/magnesium transporter (*Psat5g056120*) that contained the marker 3568469 was also found near the upper boundary of the minor QTL, *Fnw3.1* (McPhee et al., 2012). Additionally, recent validation of the actively expressed *Fop* 'secreted in xylem 4' (*Six4*) pathogenicity effector gene in pea (Ghosal & Datta, 2025) identified alpha-helices and beta-sheets encoded by *Psat1g140520* on Chr1LG6. *Six4* has also been shown to belong to the same monophyletic group within the FW species complex (Ghosal & Datta, 2025). These candidate gene functions could play a role in *Fop* defense in pea and related legumes.

5 | CONCLUSION AND FUTURE DIRECTIONS

This study provides a novel genetic dissection of pea resistance to *Fop* races 1 and 2 using a diverse panel of 324 pea

accessions. Phenotyping revealed wide quantitative variation and confirmed strong genetic control of *Fop* resistance in pea. We have also demonstrated the unprecedented quantitative inheritance of *Fop* race 1, previously considered qualitative. Wild *Pisum* relatives consistently exhibited superior *Fop* resistance, underscoring their value as reservoirs of beneficial alleles. Selected resistant accessions offer sustainable *Fop* control strategies to minimize chemical use and reduce environmental carbon footprints. The use of standardized controlled environment, coupled with rigorous phenotyping of the panel and deployment of high-throughput DArT genotyping, was valuable in mitigating poor phenotyping and genotyping bottlenecks. The use of three multi-locus GWAS models coupled with high-quality DArT markers also enhanced trait-discovery efficiency and enabled the identification of 42 robust MTAs spread across six pea chromosomes. This confirms the polygenic and race-specific nature of *Fop* resistance. Genomic hotspots were mainly detected on Chr3LG5, Chr4LG4, and Chr5LG3, while Chr1LG6, Chr2LG1, and Chr6LG2 represent novel regions for future exploration. Several MTAs colocalized with four previously reported QTLs, refining their genomic intervals and improving their precision for MAS. Particularly, marker 5929725 associated with *Psat6g017800* detected within the locus of *Fop r*ace 5 resistant gene *FwS1* is linked to *Fop* race 1 gene *Fwf* on Chr6LG2, provides a valuable validation of this region (Deng et al., 2024). This finding further demonstrates the power of GWAS to capture functionally useful gene variants and highlights the effectiveness of association studies for locating genes that may have been unnoticed in bi-parental mapping (Susmitha et al., 2023).

Thus, GWAS successfully revealed 28 candidate genes near significant DArT markers implicated in *Fop* resistance. Elucidated molecular pathways provide many transcriptional regulatory functions, vesicle trafficking, receptor-like kinases, *Fop* immune signaling, host defense genes, cell wall fortification, and detoxification in complex crosstalk for stress response to weaken pathogenic virulence. Overall, four ready to use DArT markers for *Fop* race 1 and seven for *Fop* race 2 can be deployed in MAS. Future efforts should focus on fine-mapping these genomic regions associated with *Fop* resistance and conducting functional validation of candidate genes to further bridge the genetic gap associated with major MTAs. This would serve as a springboard for clonal gene development and gene editing to guide gene insertion into elite cultivars to deliver superior varieties toward food security and reduce agrochemical use.

AUTHOR CONTRIBUTIONS

Osman Zakaria Wohor: Data curation; formal analysis; investigation; methodology; visualization; writing—original draft; writing—review and editing. **Diego Rubiales**: Conceptualization; funding acquisition; project administration; resources; supervision; writing—review and editing. **Nicolas Rispail**: Conceptualization; funding acquisition; methodology; resources; supervision; writing—review and editing.

ACKNOWLEDGMENTS

The authors would like to thank Salvador Osuna-Caballero, Miriam Marín Sanz, and Borja Rojas-Panadero for their insight and contributions to the analysis. María José Cobos is also acknowledged for technical laboratory assistance. This research was funded by the grants PID2020-113153RB-I00 and PID2023-146215OB-I00, both funded by MICIU/AEI/10.13039/501100011033 and by Horizon Europe 101081878 BELIS and 101135314 COUSIN projects. Osman Zakaria Wohor received partial PhD grant support from the Tropical Legumes III project by International Crops Research Institute for the Semi-Arid Tropics (ICRISAT).

CONFLICT OF INTEREST STATEMENT

The authors declare no conflicts of interest.

DATA AVAILABILITY STATEMENT

The genomic DArTseq marker datasets analyzed during the current study are available in the Zenodo repository, https://zenodo.org/records/7180467. Phenotypic data are available on the Table S1.

ORCID

Osman Zakaria Wohor https://orcid.org/0000-0002-7516-1074
Diego Rubiales https://orcid.org/0000-0001-9644-8616
Nicolas Rispail https://orcid.org/0000-0001-8730-0273

REFERENCES

Bani, M., Pérez-De-Luque, A., Rubiales, D., & Rispail, N. (2018). Physical and chemical barriers in root tissues contribute to quantitative resistance to *Fusarium oxysporum* f. sp. *pisi* in pea. *Frontiers in Plant Science*, *9*, 199. https://doi.org/10.3389/fpls.2018.00199

Bani, M., Rubiales, D., & Rispail, N. (2012). A detailed evaluation method to identify sources of quantitative resistance to *Fusarium oxysporum* f. sp. *pisi* race 2 within a *Pisum* spp. germplasm collection. *Plant Pathology*, *61*(3), 532–542. https://doi.org/10.1111/j.1365-3059.2011.02537.x

Berardini, T. Z., Reiser, L., Li, D., Mezheritsky, Y., Muller, R., Strait, E., & Huala, E. (2015). The Arabidopsis information resource: Making and mining the "gold standard" annotated reference plant genome. *Genesis*, *53*(8), 474–485.

Berka, M., Kopecká, R., Berková, V., Brzobohatý, B., & Černý, M. (2022). Regulation of heat shock proteins 70 and their role in plant immunity. *Journal of Experimental Botany*, *73*(7), 1894–1909. https://doi.org/10.1093/jxb/erab549

Bland, J. M., & Altman, D. G. (1995). Multiple significance tests: The Bonferroni method. *Bmj*, *310*(6973), 170.

Bogamuwa, S. P., & Jang, J. C. (2014). Tandem CCCH zinc finger proteins in plant growth, development and stress response. *Plant and Cell Physiology*, *55*(8), 1367–1375. https://doi.org/10.1093/pcp/pcu074

Chen, M., Galvão, R. M., Li, M., Burger, B., Bugea, J., Bolado, J., & Chory, J. (2010). Arabidopsis HEMERA/pTAC12 initiates photomorphogenesis by phytochromes. *Cell*, *141*(7), 1230–1240.

Cheung, A. Y. (2024). FERONIA: A receptor kinase at the core of a global signaling network. *Annual Review of Plant Biology*, *75*, 345–375. https://doi.org/10.1146/annurev-arplant-102820-103424

Coyne, C. J., Inglis, D. A., Whitehead, S. J., McClendon, M. T., & Muehlbauer, F. J. (2000). Chromosomal location of *Fwf*, the Fusarium wilt race 5 resistance gene in *Pisum sativum*. *Pisum Genetics*, *32*, 20–22.

Crosta, M., Romani, M., Nazzicari, N., Ferrari, B., & Annicchiarico, P. (2023). Genomic prediction and allele mining of agronomic and morphological traits in pea (*Pisum sativum*) germplasm collections. *Frontiers in Plant Science*, *14*, 1320506. https://doi.org/10.3389/fpls.2023.1320506

De la Concepcion, J. C. (2023). The exocyst complex is an evolutionary battleground in plant-microbe interactions. *Current Opinion in Plant Biology*, *76*, 102482.

Deng, D., Sun, S., Wu, W., Duan, C., Wu, X., & Zhu, Z. (2024). Fine mapping and identification of a Fusarium wilt resistance gene *FwS1* in pea. *Theoretical and Applied Genetics*, *137*(7), 171. https://doi.org/10.1007/s00122-024-04682-1

Deng, D., Sun, S., Wu, W., Zong, X., Yang, X., Zhang, X., He, Y., Duan, C., & Zhu, Z. (2022). Screening for pea germplasms resistant to Fusarium wilt race 5. *Agronomy*, *12*(6), 1354. https://doi.org/10.3390/agronomy12061354

de Resende, M. D. V., Silva, F. F., Resende, M. F. R., & Azevedo, C. F. (2014). Genome-wide association studies (GWAS). In A. Borém, & R. Fritsche-Neto (Eds.), *Biotechnology and plant breeding: Applications and approaches for developing improved cultivars* (pp. 83–104). Elsevier.

Desgroux, A., L'Anthoëne, V., Roux-Duparque, M., Rivière, J.-P., Aubert, G., Tayeh, N., Moussart, A., Mangin, P., Vetel, P., Piriou, C., Mcgee, R. J., Coyne, C. J., Burstin, J., Baranger, A., Manzanares-Dauleux, M., Bourion, V., & Pilet-Nayel, M.-L. (2016). Genome-wide association mapping of partial resistance to *Aphanomyces euteiches* in pea. *BMC Genomics*, *17*, Article 124. https://doi.org/10.1186/s12864-0162429-4

Devlin, B., & Roeder, K. (1999). Genomic control for association studies. *Biometrics*, *55*, 997–1004. https://doi.org/10.1111/j.0006-341x.1999.00997.x

FAOSTAT. (2025). *Crops and livestock products*. Food and Agriculture Organization of the United Nations. http://www.fao.org/faostat/en/#data/QC

Gali, K. K., Liu, Y., Sindhu, A., Diapari, M., Shunmugam, A. S. K., Arganosa, G., Daba, K., Caron, C., Lachagari, R. V. B., Tar'an, B., & Warkentin, T. D. (2018). Construction of high-density linkage maps for mapping quantitative trait loci for multiple traits in field pea (*Pisum sativum* L.). *BMC Plant Biology*, *18*, 1–25. https://doi.org/10.1186/s12870-018-1368-4

Gali, K. K., Sackville, A., Tafesse, E. G., Lachagari, V. B. R., Mcphee, K., Hybl, M., Mikić, A., Smýkal, P., Mcgee, R., Burstin, J., Domoney, C., Ellis, T. H. N., Tar'an, B., & Warkentin, T. D. (2019). Genome-wide association mapping for agronomic and seed quality traits of field pea (*Pisum sativum* L.). *Frontiers in Plant Science*, *10*, 1538. https://doi.org/10.3389/fpls.2019.01538

Gali, K. K., Tar'an, B., Madoui, M.-A., Van Der Vossen, E., Van Oeveren, J., Labadie, K., Berges, H., Bendahmane, A., Lachagari, R. V. B., Burstin, J., & Warkentin, T. (2019). Development of a sequence-based reference physical map of pea (*Pisum sativum* L.). *Frontiers in Plant Science*, *10*, 323. https://doi.org/10.3389/fpls.2019.00323

Ghosal, D., & Datta, B. (2025). Molecular characterization and in silico analysis of 'secreted in xylem 4' (Six4) gene from *Fusarium oxysporum* infecting *Pisum sativum*. *Archives of Microbiology*, *207*, 337. https://doi.org/10.1007/s00203-025-04545-3

Hoagland, D. R., & Arnon, D. I. (1938). The water-culture method for growing plants without soil. *California Agricultural Experiment Station Circular*, *347*, 1–39.

Hoffmann, C., Plocharski, B., Haferkamp, I., Leroch, M., Ewald, R., Bauwe, H., Riemer, J., Herrmann, J. M., & Neuhaus, H. E. (2013). From endoplasmic reticulum to mitochondria: Absence of the Arabidopsis ATP antiporter endoplasmic reticulum adenylate transporter1 perturbs photorespiration. *The Plant Cell*, *25*(7), 2647–2660.

Huang, M., Liu, X., Zhou, Y., Summers, R. M., & Zhang, Z. (2019). BLINK: A package for the next level of genome-wide association studies with both individuals and markers in the millions. *Gigascience*, *8*(2), giy154.

Huebbers, J. W., Caldarescu, G. A., Kubátová, Z., Sabol, P., Levecque, S. C. J., Kuhn, H., Kulich, I., Reinstädler, A., Büttgen, K., Manga-Robles, A., Mélida, H., Pauly, M., Panstruga, R., & Žárský, V. (2024). Interplay of EXO70 and MLO proteins modulates trichome cell wall composition and susceptibility to powdery mildew. *The Plant Cell*, *36*(4), 1007–1035. https://doi.org/10.1093/plcell/koad319

Infantino, A., Kharrat, M., Riccioni, L., Coyne, C. J., McPhee, K. E., & Grünwald, N. J. (2006). Screening techniques and sources of resistance to root diseases in cool season food legumes. *Euphytica*, *147*, 201–221. https://doi.org/10.1007/s10681-006-6963-z

Jain, S., Weeden, N. F., Kumar, A., Chittem, K., & McPhee, K. (2015). Functional codominant marker for selecting the *Fw* gene conferring resistance to Fusarium wilt race 1 in pea. *Crop Science*, *55*(6), 2639–2646. https://doi.org/10.2135/cropsci2015.02.0102

Jombart, T. (2008). adegenet: A R package for the multivariate analysis of genetic markers. *Bioinformatics*, *24*(11), 1403–1405. https://doi.org/10.1093/bioinformatics/btn129

Jombart, T., Devillard, S., & Balloux, F. (2010). Discriminant analysis of principal components: A new method for the analysis of genetically structured populations. *BMC Genetics*, *11*, Article 94. http://doi.org/10.1186/1471-2156-11-94

Kassambara, A. (2023). rstatix: Pipe-Friendly Framework for Basic Statistical Tests (R package version 0.7. 2). https://cran.r-project.org/web/packages/rstatix/index.html

Klink, V. P., Lawaju, B. R., Niraula, P. M., Sharma, K., Mcneece, B. T., Pant, S. R., Troell, H. A., Acharya, S., Khatri, R., Rose, A. H., Alkharouf, N. W., & Lawrence, K. S. (2022). The conserved oligomeric Golgi (COG) complex, a window into plant-pathogen interactions. *Journal of Plant Interactions*, *17*(1), 344–360. https://doi.org/10.1080/17429145.2022.2041743

Kreplak, J., Madoui, M.-A., Cápal, P., Novák, P., Labadie, K., Aubert, G., Bayer, P. E., Gali, K. K., Syme, R. A., Main, D., Klein, A., Bérard, A., Vrbová, I., Fournier, C., d'Agata, L., Belser, C., Berrabah, W., Toegelová, H., Milec, Z., … Burstin, J. (2019). A reference genome for pea provides insight into legume genome evolution. *Nature Genetics*, *51*(9), 1411–1422. https://doi.org/10.1038/s41588-019-0480-1

Lao, J., Oikawa, A., Bromley, J. R., Mcinerney, P., Suttangkakul, A., Smith-Moritz, A. M., Plahar, H., Chiu, T.-Y., González Fernández-Niño, S. M., Ebert, B., Yang, F., Christiansen, K. M., Hansen, S. F.,

Stonebloom, S., Adams, P. D., Ronald, P. C., Hillson, N. J., Hadi, M. Z., Vega-Sánchez, M. E., … Heazlewood, J. L. (2014). The plant glycosyltransferase clone collection for functional genomics. *The Plant Journal*, *79*(3), 517–529.

Lashbrooke, J., Cohen, H., Levy-Samocha, D., Tzfadia, O., Panizel, I., Zeisler, V., Massalha, H., Stern, A., Trainotti, L., Schreiber, L., Costa, F., & Aharoni, A. (2016). MYB107 and MYB9 homologs regulate suberin deposition in angiosperms. *The Plant Cell*, *28*(9), 2097–2116. https://doi.org/10.1105/tpc.16.00490

Leprévost, T., Boutet, G., Lesné, A., Rivière, J.-P., Vetel, P., Glory, I., Miteul, H., Le Rat, A., Dufour, P., Regnault-Kraut, C., Sugio, A., Lavaud, C., & Pilet-Nayel, M.-L. (2023). Advanced backcross QTL analysis and comparative mapping with RIL QTL studies and GWAS provide an overview of QTL and marker haplotype diversity for resistance to Aphanomyces root rot in pea (*Pisum sativum*). *Frontiers in Plant Science*, *14*, 1189289. https://doi.org/10.3389/fpls.2023.1189289

Li, Y., Chen, H., Chen, W., Gu, J., Yuan, J., Li, C., Lin, Y., Lu, P., Wang, T., Li, Y., Lee, D., Ye, H., Nguyen, H. T., & Wang, Z. Y. (2026). Identification of genetic loci and domestication gene GmZFP1 associated with soybean hypocotyl elongation in seedling stage by genome-wide association study. *BMC Plant Biology*, *26*, Aticle 215. http://doi.org/10.1186/s12870-025-08052-x

Liu, N., Lyu, X., Zhang, X., Zhang, G., Zhang, Z., Guan, X., Chen, X., Yang, X., Feng, Z., Gao, Q., Shi, W., Deng, Y., Sheng, K., Ou, J., Zhu, Y., Wang, B., Bu, Y., Zhang, M., Zhang, L., … Gong, Y. (2024). Reference genome sequence and population genomic analysis of peas provide insights into the genetic basis of Mendelian and other agronomic traits. *Nature Genetics*, *56*(9), 1964–1974. https://doi.org/10.1038/s41588-024-01867-8

Liu, X., Huang, M., Fan, B., Buckler, E. S., & Zhang, Z. (2016). Iterative usage of fixed and random effect models for powerful and efficient genome-wide association studies. *PLoS Genetics*, *12*(2), e1005767.

Liu, X., Zhang, H., Ma, L., Wang, Z., & Wang, K. (2020). Genome-wide identification and expression profiling analysis of the trihelix gene family under abiotic stresses in *Medicago truncatula*. *Genes*, *11*(11), 1389. https://doi.org/10.3390/genes11111389

Masachis, S., Segorbe, D., Turrà, D., Leon-Ruiz, M., Fürst, U., El Ghalid, M., Leonard, G., López-Berges, M. S., Richards, T. A., Felix, G., & Di Pietro, A. (2016). A fungal pathogen secretes plant alkalinizing peptides to increase infection. *Nature Microbiology*, *1*(6), 1–9. https://doi.org/10.1038/nmicrobiol.2016.43

McClendon, M. T., Inglis, D. A., McPhee, K. E., & Coyne, C. J. (2002). DNA markers linked to Fusarium wilt race 1 resistance in pea. *Journal of the American Society for Horticultural Science*, *127*, 602–607.

Mc Phee, K. E., Inglis, D. A., Gundersen, B., & Coyne, C. J. (2012). Mapping QTL for Fusarium wilt race 2 partial resistance in pea (*Pisum sativum*). *Plant Breeding*, *131*(2), 300–306. https://doi.org/10.1111/j.1439-0523.2011.01938.x

McPhee, K. E., Tullu, A., Kraft, J. M., & Muehlbauer, F. J. (1999). Resistance to Fusarium wilt race 2 in the *Pisum* core collection. *Journal of the American Society for Horticultural Science*, *124*(1), 28–31. https://doi.org/10.21273/JASHS.124.1.28

Myles, C., & Wayne, M. (2008). Quantitative trait locus (QTL) analysis. *Nature Education*, *1*(1), 208.

Neumann, S., & Xue, A. G. (2003). Reactions of field pea cultivars to four races of *Fusarium oxysporum* f. sp. *pisi*. *Canadian Journal of Plant Science*, *83*(2), 377–379. https://doi.org/10.4141/P02-048

Nogué, F., Mara, K., Collonnier, C., & Casacuberta, J. M. (2016). Genome engineering and plant breeding: Impact on trait discovery and development. *Plant Cell Reports*, *35*, 1475–1486. https://doi.org/10.1007/s00299-016-1993-z

Nunes-Nesi, A., Cavalcanti, J. H. F., & Fernie, A. R. (2020). Characterization of in vivo function(s) of members of the plant mitochondrial carrier family. *Biomolecules*, *10*(9), 1226. https://doi.org/10.3390/biom10091226

Olivoto, T., & Lúcio, A. D. C. (2020). metan: An R package for multi-environment trial analysis. *Methods in Ecology and Evolution*, *11*(6), 783–789. https://doi.org/10.1111/2041-210x.13384

Ortiz-Morea, F. A., Liu, J., Shan, L., & He, P. (2022). Malectin-like receptor kinases as protector deities in plant immunity. *Nature Plants*, *8*(1), 27–37. https://doi.org/10.1038/s41477-021-01028-3

Osuna-Caballero, S., Cobos, M. J., Ruiz, C. M., Wohor, O. Z., Rispail, N., & Rubiales, D. (2024a). Genome-wide association studies on resistance to pea weevil: Identification of novel sources of resistance and associated markers. *International Journal of Molecular Sciences*, *25*(14), 7920. https://doi.org/10.3390/ijms25147920

Osuna-Caballero, S., Rubiales, D., & Rispail, N. (2024b). Genome-wide association study uncovers pea candidate genes and metabolic pathways involved in rust resistance. *The Plant Genome*, *17*(4), e20510. https://doi.org/10.1002/tpg2.20510

Pandey, A. K., Rubiales, D., Wang, Y., Fang, P., Sun, T., Liu, N., & Xu, P. (2021). Omics resources and omics-enabled approaches for achieving high productivity and improved quality in pea (*Pisum sativum* L.). *Theoretical and Applied Genetics*, *134*, 755–776. https://doi.org/10.1007/s00122-020-03751-5

Piepho, H. P., & Möhring, J. (2007). Computing heritability and selection response from unbalanced plant breeding trials. *Genetics*, *177*(3), 1881–1888. https://doi.org/10.1534/genetics.107.074229

Porter, L. D., Kraft, J. M., & Grünwald, N. J. (2014). Release of pea germplasm with Fusarium resistance combined with desirable yield and anti-lodging traits. *Journal of Plant Registrations*, *8*(2), 191–194. https://doi.org/10.3198/jpr2013.07.0041crg

Qiu, Y., Li, M., Pasoreck, E. K., Long, L., Shi, Y., Galvão, R. M., Chou, C. L., Wang, H., Sun, A. Y., Zhang, Y. C., Jiang, A., & Chen, M. (2015). HEMERA couples the proteolysis and transcriptional activity of PHYTOCHROME INTERACTING FACTORs in Arabidopsis photomorphogenesis. *The Plant Cell*, *27*(5), 1409–1427.

R Core Team. (2024). *R: A language and environment for statistical computing*. R Foundation for Statistical. https://www.R-project.org

Rigden, D. J. (2019). Protein phosphohistidine phosphatases of the HP superfamily. In *Histidine phosphorylation: Methods and protocols* (pp. 93–107). Springer US.

Rispail, N., Wohor, O. Z., Osuna-Caballero, S., Barilli, E., & Rubiales, D. (2022). *Dataset for genetic diversity and population structure of a wide Pisum spp. core collection*. Zenodo. https://doi.org/10.5281/zenodo.7180467

Rispail, N., Wohor, O. Z., Osuna-Caballero, S., Barilli, E., & Rubiales, D. (2023). Genetic diversity and population structure of a wide *Pisum* spp. core collection. *International Journal of Molecular Sciences*, *24*(3), 2470. https://doi.org/10.3390/ijms24032470

Robinson, G. K. (1991). That BLUP is a good thing: The estimation of random effects. *Statistical Science*, *6*, 15–32. https://doi.org/10.1214/ss/1177011926

Rodriguez-Mena, S., Vaz Patto, M. C., Leitão, S. T., Rubiales, D., & González, M. (2025). Identification of genomic regions associated

with partial resistance to Aphanomyces root rot in pea. *The Plant Genome*, *18*, e70164. https://doi.org/10.1002/tpg2.70164

Rubiales, D. (2023). Plant breeding is needed to meet agroecological requirements: Legume crops as a case study. *Outlook on Agriculture*, *52*(3), 294–302. https://doi.org/10.1177/00307270231195641

Rubiales, D., Barilli, E., & Rispail, N. (2023). Breeding for biotic stress resistance in pea. *Agriculture*, *13*(9), 1825. https://doi.org/10.3390/agriculture13091825

Rubiales, D., González-Bernal, M. J., Warkentin, T., Bueckert, R., Patto, M. C. V., McPhee, K., McGee, R., & Smykal, P. (2019). Advances in pea breeding. In *Achieving sustainable cultivation of vegetables* (pp. 575–606). Burleigh Dodds Science Publishing.

Sampaio, A. M., Alves, M. L., Pereira, P., Valiollahi, E., Santos, C., Šatović, Z., Rubiales, D., Araújo, S. D. S., Van Eeuwijk, F., & Vaz Patto, M. C. (2021). Grass pea natural variation reveals oligogenic resistance to *Fusarium oxysporum* f. sp. *pisi*. *The Plant Genome*, *14*(3), e20154. https://doi.org/10.1002/tpg2.20154

Sindhu, A., Ramsay, L., Sanderson, L.-A., Stonehouse, R., Li, R., Condie, J., Shunmugam, A. S. K., Liu, Y., Jha, A. B., Diapari, M., Burstin, J., Aubert, G., Tar'an, B., Bett, K. E., Warkentin, T. D., & Sharpe, A. G. (2014). Gene-based SNP discovery and genetic mapping in pea. *Theoretical and Applied Genetics*, *127*, 2225–2241. https://doi.org/10.1007/s00122-014-2375-y

Singh, G., Gudi, S., Amandeep, Upadhyay, P., Shekhawat, P. K., Nayak, G., Goyal, L., Kumar, D., Kumar, P., Kamboj, A., Thada, A., Shekhar, S., Koli, G. K., Dp, M., Halladakeri, P., Kaur, R., Kumar, S., Saini, P., Singh, I., & Ayoubi, H. (2022). Unlocking the hidden variation from wild repository for accelerating genetic gain in legumes. *Frontiers in Plant Science*, *13*, 1035878. https://doi.org/10.3389/fpls.2022.1035878

Smýkal, P., Aubert, G., Burstin, J., Coyne, C. J., Ellis, N. T., Flavell, A. J., Ford, R., Hýbl, M., Macas, J., Neumann, P., McPhee, K. E., Redden, R. J., Rubiales, D., Weller, J. L., & Warkentin, T. D. (2012). Pea (*Pisum sativum* L.) in the genomic era. *Agronomy*, *2*(2), 74–115. http://doi.org/10.3390/agronomy2020074

Storey, J. D., Bass, A. J., Dabney, A., & Robinson, D. (2024). qvalue: Q-Value Estimation for False Discovery Rate Control. (R package version 2.36. 0.). http://github.com/jdstorey/qvalue

Susmitha, P., Kumar, P., Yadav, P., Sahoo, S., Kaur, G., Pandey, M. K., Singh, V., Tseng, T. M., & Gangurde, S. S. (2023). Genome-wide association study as a powerful tool for dissecting competitive traits in legumes. *Frontiers in Plant Science*, *14*, 1123631. https://doi.org/10.3389/fpls.2023.1123631

Tayeh, N., Aubert, G., Pilet-Nayel, M. L., Lejeune-Hénaut, I., Warkentin, T. D., & Burstin, J. (2015). Genomic tools in pea breeding programs: Status and perspectives. *Frontiers in Plant Science*, *6*, 1037. https://doi.org/10.3389/fpls.2015.01037

van Damme, M., Zeilmaker, T., Elberse, J., Andel, A., de Sain-van der Velden, M., & van den Ackerveken, G. (2009). Downy mildew resistance in Arabidopsis by mutation of HOMOSERINE KINASE. *The Plant Cell*, *21*(7), 2179–2189. https://doi.org/10.1105/tpc.109.066811

Verma, N., Yadav, S., Rana, N., Maheshwari, R., Kaur, M., Kumari, P., Kumar, P., Dhall, R. K., Singh, H., Sharma, P., & Chunneja, P. (2025). Genetic and molecular approaches for Fusarium wilt resistance in garden pea: Advances and future outlook. *Plant Molecular Biology*, *115*, 89. https://doi.org/10.1007/s11103-025-01624-3

Wang, J., Tang, Y., & Zhang, Z. (2022). Performing genome-wide association studies with multiple models using GAPIT. In D. Torkamaneh & F. Belzile (Eds.), *Genome-wide association studies* (pp. 199–217). Humana. https://doi.org/10.1007/978-1-0716-2237-7_13

Wang, J., & Zhang, Z. (2021). GAPIT version 3: Boosting power and accuracy for genomic association and prediction. *Genomics, Proteomics & Bioinformatics*, *19*(4), 629–640. https://doi.org/10.1016/j.gpb.2021.08.005

Wang, Q. (2016). QQperm: Permutation Based QQ Plot and Inflation Factor Estimation (R package version 1.0.1.) https://cran.r-project.org/web/packages/QQperm

Windsor, N., Boatwright, L., Boyles, R., Bridges, W., Rubiales, D., & Thavarajah, D. (2024). Characterizing dry pea (*Pisum sativum* L.) for improved nutritional traits and the potential for biofortification. *Legume Science*, *6*(3), e250. https://doi.org/10.1002/leg3.250

Wohor, O. Z., Rispail, N., Ojiewo, C. O., & Rubiales, D. (2022). Pea breeding for resistance to rhizospheric pathogens. *Plants*, *11*(19), 2664. https://doi.org/10.3390/plants11192664

Wohor, O. Z., Rispail, N., & Rubiales, D. (2025). Genome wide association study unveils the genetic basis of *Orobanche crenata* resistance in pea. *Theoretical and Applied Genetics*, *138*, 272. https://doi.org/10.1007/s00122-025-05051-2

Xu, J., Huang, Z., Du, H., Tang, M., Fan, P., Yu, J., & Zhou, Y. (2023). SEC1-C3H39 module fine-tunes cold tolerance by mediating its target mRNA degradation in tomato. *New Phytologist*, *237*(3), 870–884. https://doi.org/10.1111/nph.18568

Yang, T., Liu, R., Luo, Y., Hu, S., Wang, D., Wang, C., Pandey, M. K., Ge, S., Xu, Q., Li, N., Li, G., Huang, Y., Saxena, R. K., Ji, Y., Li, M., Yan, X., He, Y., Liu, Y., Wang, X., … Zong, X. (2022). Improved pea reference genome and pan-genome highlight genomic features and evolutionary characteristics. *Nature Genetics*, *54*(10), 1553–1563. https://doi.org/10.1038/s41588-022-01172-2

Yanhui, C., Xiaoyuan, Y., Kun, H., Meihua, L., Jigang, L., Zhaofeng, G., Zhiqiang, L., Yunfei, Z., Xiaoxiao, W., Xiaoming, Q., Yunping, S., Li, Z., Xiaohui, D., Jingchu, L., Xing-Wang, D., Zhangliang, C., Hongya, G., & Li-Jia, Q. (2006). The MYB transcription factor superfamily of Arabidopsis: Expression analysis and phylogenetic comparison with the rice MYB family. *Plant Molecular Biology*, *60*, 107–124. https://doi.org/10.1007/s11103-005-2910-y

Yin, L., Zhang, H., Tang, Z., Xu, J., Yin, D., Zhang, Z., Yuan, X., Zhu, M., Zhao, S., Li, X., & Liu, X. (2021). rMVP: A memory-efficient, visualization-enhanced, and parallel-accelerated tool for genome-wide association study. *Genomics, Proteomics & Bioinformatics*, *19*(4), 619–628. https://doi.org/10.1016/j.gpb.2020.10.007

Yu, J., Pressoir, G., Briggs, W. H., Vroh Bi, I., Yamasaki, M., Doebley, J. F., Mcmullen, M. D., Gaut, B. S., Nielsen, D. M., Holland, J. B., Kresovich, S., & Buckler, E. S. (2006). A unified mixed-model method for association mapping that accounts for multiple levels of relatedness. *Nature Genetics*, *38*(2), 203–208. https://doi.org/10.1038/ng1702

Zander, P., Amjath-Babu, T. S., Preissel, S., Reckling, M., Bues, A., Schläfke, N., Kuhlman, T., Bachinger, J., Uthes, S., Stoddard, F., Murphy-Bokern, D., & Watson, C. (2016). Grain legume decline and potential recovery in European agriculture: A review. *Agronomy for Sustainable Development*, *36*, 1–20. https://doi.org/10.1007/s13593-016-0365-y

Zhang, X., Pumplin, N., Ivanov, S., & Harrison, M. J. (2015). EXO70I is required for development of a sub-domain of the periarbuscular membrane during arbuscular mycorrhizal symbiosis. *Current Biology*, *25*(16), 2189–2195. https://doi.org/10.1016/j.cub.2015.06.075

SUPPORTING INFORMATION

Additional supporting information can be found online in the Supporting Information section at the end of this article.

How to cite this article: Wohor, O. Z., Rubiales, D., & Rispail, N. (2026). Genome-wide association studies of a pea germplasm reveal novel markers and candidate genes implicated in resistance to *Fusarium oxysporum* f. sp. *pisi* races 1 and 2. *The Plant Genome*, *19*, e70250. https://doi.org/10.1002/tpg2.70250